



GEOLOGICAL SURVEY OF CANADA
COMMISSION GÉOLOGIQUE DU CANADA

PAPER 75-17

This document was produced
by scanning the original publication.

Ce document est le produit d'une
numérisation par balayage
de la publication originale.

**GEOLOGY AND HYDROTHERMAL
ALTERATION AT THE MAGGIE PORPHYRY
COPPER-MOLYBDENUM DEPOSIT,
SOUTH-CENTRAL, BRITISH COLUMBIA**

J.L. JAMBOR





**GEOLOGICAL SURVEY
PAPER 75-17**

**GEOLOGY AND HYDROTHERMAL
ALTERATION AT THE MAGGIE PORPHYRY
COPPER-MOLYBDENUM DEPOSIT,
SOUTH-CENTRAL, BRITISH COLUMBIA**

J.L. JAMBOR

1976

© Minister of Supply and Services Canada 1976

Available by mail from

Printing and Publishing
Supply and Services Canada,
Ottawa, Canada K1A 0S9

from the Geological Survey of Canada
601 Booth St., Ottawa, K1A 0E8

and at Canadian Government Bookstores:

HALIFAX
1683 Barrington Street

MONTREAL
640 St. Catherine Street West

OTTAWA
171 Slater Street

TORONTO
221 Yonge Street

WINNIPEG
393 Portage Avenue

VANCOUVER
800 Granville Street

or through your bookseller

Catalogue No. M44-75-17 Price: Canada: \$3.00
Other Countries: \$3.60

Price subject to change without notice

CONTENTS

	Page
Abstract/Résumé	v
Introduction	1
Acknowledgments	3
General Geology	3
Porphyry intrusions	4
Porphyritic diorite and quartz diorite	4
Quartz monzonite porphyry	5
Megascopic subdivisions of the quartz monzonite porphyry intrusion	6
Microscopic subdivisions of the quartz monzonite porphyry intrusion	7
Finer grained quartz monzonite porphyry and associated breccias	9
Sulphide mineralization	10
Pyrite	10
Ore minerals	12
Hydrothermal alteration	13
Hydrothermal biotitization	15
Biotite compositions	16
Biotite quality in relation to copper grades	17
K-feldspar alteration	17
Silicification and sericitization	20
Argillic alteration	23
Carbonate alteration	24
Supergene alteration	24
Conclusions	24
References	24
Appendix I: Microprobe analyses of biotites from Maggie deposit	
Descriptive notes	27
Microprobe analyses	30

Tables

Table 1. Chemical analyses of diorite and quartz monzonite porphyry intrusions, Maggie deposit	5
2. Characterization of hydrothermal biotites in terms of quality	13
3. Comparison of maximum pleochroic colours of biotites and their Fe/Fe+Mg+Mn ratios	16
4. Clay mineral ratios in Maggie samples	18

Illustrations

Figure 1. Location map	1
2. Geology of the Maggie property	2
3. Location of the diamond-drill holes of Bethlehem Copper	3
4. Photographs of diorite and quartz diorite porphyry from the Maggie deposit	4
5. Photomicrographs of diorite and quartz diorite porphyry	6
6. Position of the porphyritic intrusions as determined megascopically ...	7
7. Photographs of drill-core specimens of the quartz monzonite porphyry	8
8. Photographs of drill-core specimens of quartz monzonite porphyry and breccia	9
9. Photomicrographs of hydrothermal biotite	10
10. Comparison of megascopic and microscopic subdivisions of the quartz monzonite porphyry	11
11. Example of poor correlation between the megascopic and microscopic subdivisions of the porphyry	12
12. Photomicrographs of the quartz monzonite porphyry	14

Figure 13. Distribution of the fine grained porphyry as determined microscopically	15
14. Cross-section distribution of the fine grained porphyry	16
15. Relative abundance of pyrite in the Maggie deposit drillholes	17
16. Tennantite occurrences	17
17. Distribution of hydrothermal biotite	18
18. Drillhole locations of biotites analyzed by microprobe	18
19. Fe/Fe+Mg+Mn versus Ti in biotites from the Maggie deposit	19
20. Estimated distribution of the +0.2% Cu zone in longitudinal section	20
21. Estimated distribution of the +0.2% Cu zone in longitudinal section	21
22. Estimated distribution of the +0.2% Cu zone in longitudinal section	22
23. Estimated distribution of the +0.2% Cu zone in longitudinal section	22
24. Distribution and relative abundance of quartz veining and silicification in the Maggie deposit drillholes	23
25. Distribution of calcite and dolomite in the Maggie deposit drillholes ...	23

GEOLOGY AND HYDROTHERMAL ALTERATION AT THE MAGGIE PORPHYRY COPPER-MOLYBDENUM DEPOSIT, SOUTH-CENTRAL BRITISH COLUMBIA

Abstract

The Maggie porphyry copper deposit is associated with early Tertiary porphyries that intrude for the most part the Permian Cache Creek Group. The copper-molybdenum zone, approximately 1300 by 300 metres in surface dimensions, averages about 0.28% Cu. The zone is centred in an elongate, westerly-dipping, multi-phase intrusive body that ranges in composition from granodioritic to granitic. Because abundant, conspicuous K-feldspar phenocrysts are present, the pluton is referred to as quartz monzonite porphyry.

From the centre outwards the succession of copper sulphides is (1) chalcopyrite with very minor bornite, (2) chalcopyrite, (3) chalcopyrite \pm tennantite. Pyrite is present in all zones, but is most abundant in an irregularly-shaped, elongate halo that encloses the copper zone. Hydrothermal biotite is associated closely with the copper sulphides, and because assay data were not available, the quality of biotitization has been used to establish the probable limits of 0.2% Cu in several cross-sections. Microprobe analyses of numerous biotites indicate that their colour deepens (and quality improves) as Fe/Fe+Mg+Mn increases. Biotitization is succeeded outwards by sericitization; along parts of the hanging wall of the deposit, intense sericitic alteration is accompanied by pervasive silicification. Propylitic alteration is present outside the zone of sericitization, but in Cache Creek rocks such alteration is difficult to distinguish from the effects of low-grade regional metamorphism.

Résumé

Le gisement de porphyres cuprifères de Maggie est associé avec des porphyres du début du Tertiaire, qui, pour la plupart, ont fait intrusion dans le groupe de Cache Creek du Permien. La zone où l'on trouve du cuivre et du molybdène, qui forme, en gros, un rectangle de 1300 par 300 mètres de côté, a une teneur moyenne en cuivre d'environ 0.28 p. cent. La zone est au centre d'une masse intrusive oblongue hétérogène, plongeant vers l'ouest. Les roches de cette intrusion vont des granodiorites aux granites. Du fait de la présence en abondance de phénocristaux très apparents de feldspaths potassiques, la masse plutonique est qualifiée de monzonite quartzique porphyrique.

En allant du centre vers l'extérieur, la suite des sulfures de cuivre est la suivante: (1) chalcopyrite avec une très faible quantité de bornite, (2) chalcopyrite, (3) chalcopyrite avec plus ou moins de tennantite. La pyrite est présente partout, mais elle est la plus abondante dans une auréole allongée, de forme irrégulière, qui entoure la zone cuprifère. De la biotite d'origine hydrothermale est intimement associée aux sulfures de cuivre et, comme l'auteur ne disposait pas des résultats des analyses, il s'est servi de la formation des biotites et de leur qualité pour établir, sur plusieurs coupes, la limite probable de la zone des teneurs en cuivre supérieures à 0.2 p. cent. L'analyse à la microsonde de nombreuses biotites indique que leur couleur est de plus en plus foncée (donc que leur qualité s'améliore) quand le rapport Fe/Fe+Mg+Mn augmente. A la formation de biotite, succède, en allant, vers l'extérieur, la séricitisation; en certaines parties du toit du gisement, la séricitisation est accompagnée d'une silicification pénétrante. Il y a eu propylitisation à l'extérieur de la zone de séricitisation, mais dans les roches de Cache Creek, cette altération est difficile à distinguer des effets du métamorphisme régional de degré peu élevé.

GEOLOGY AND HYDROTHERMAL ALTERATION AT THE MAGGIE PORPHYRY COPPER-MOLYBDENUM DEPOSIT,
SOUTH-CENTRAL BRITISH COLUMBIA

INTRODUCTION

The Maggie porphyry copper deposit in south-central British Columbia (Fig. 1) is about fifteen miles north-northwest of Ashcroft, and about thirty-five miles northwest of the Highland Valley copper deposits. Drilling by Bethlehem Copper Corporation has outlined a porphyry deposit containing about 200 million tons of approximately 0.28% Cu and 0.029% Mo¹. The Cu-Mo zone is covered by 125-360 feet of overburden, but there is an extremely prominent gossan on a pyrite halo that outcrops on hills surrounding the copper zone. The Maggie property is cut by the valley of the Bonaparte River and is traversed by Highway 97 (Fig. 2).

Interest in the deposit dates to about the turn of the century. A shaft near the northern periphery of the pyrite halo marks the site of underground exploration

started before 1907. The workings followed quartz-pyrite-chalcopyrite lenses that occurred along a southwesterly-striking fault zone that dips about 70° south. In the British Columbia Department of Mines Annual Report for 1907, it is stated that 45 to 50 tons of ore containing 8 per cent Cu and 2 ounces Ag per ton were shipped from workings which at that time consisted of three levels with access from an adit and shaft. However, little subsequent work was done.

In about 1952, Kennecott Copper drilled three holes, believed to be near the workings, and in 1964 Frobex Ltd. drilled at least three widely-spaced holes in the western portion of the pyrite halo. Bethlehem Copper Corporation did percussion drilling in 1968, and in the following year diamond-drilled a hole 1487 feet deep (D.D.H. 1, Fig. 3). Although collared in the pyrite halo, the hole at depth intersected the encouraging

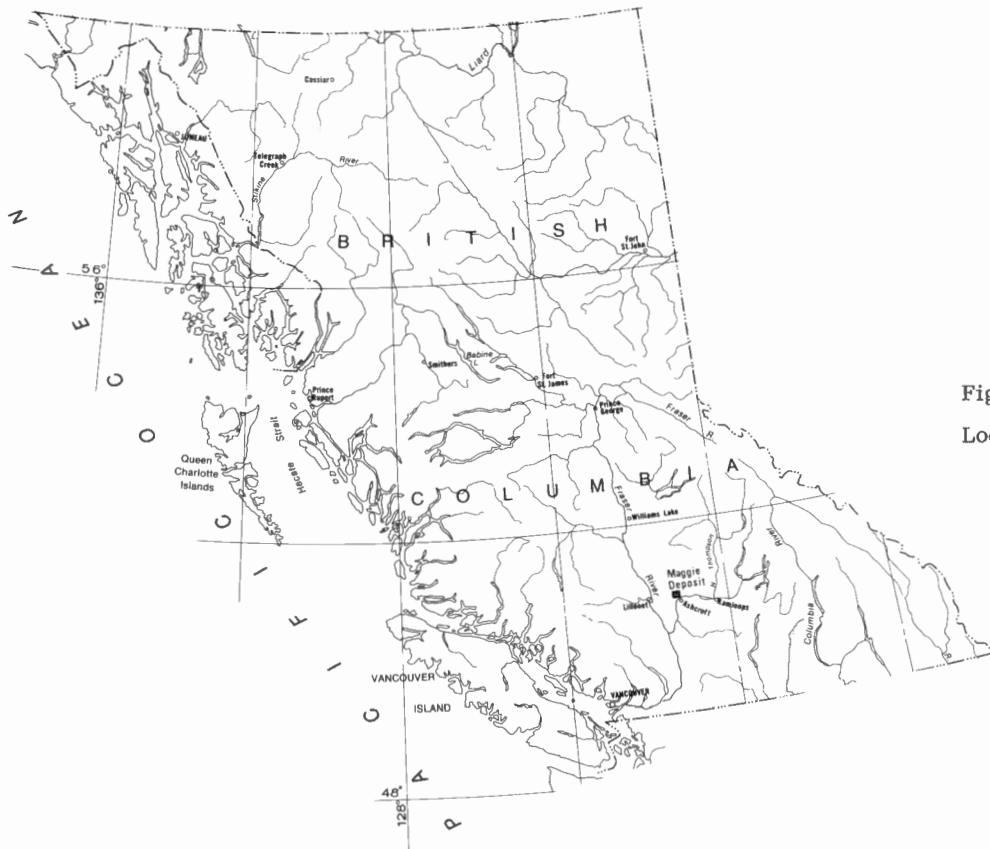


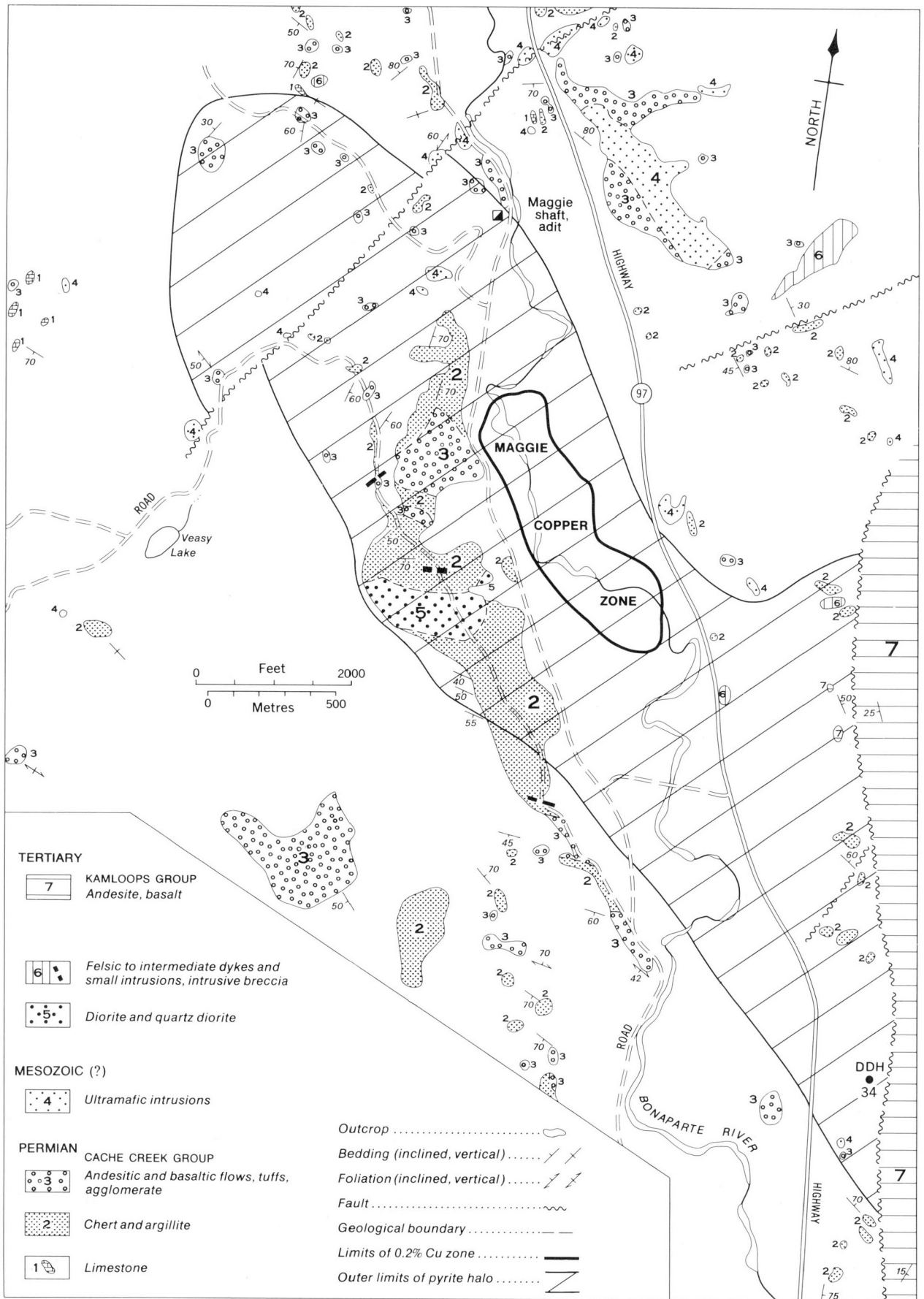
Figure 1
Location map.

¹ Annual reports of the company generally state the grade to be about 0.4% copper equivalent. Reserves given above were kindly provided by the company (personal communication, January 1976).

² Author's present address: CANMET, Dept. Energy, Mines and Resources, 555 Booth St., Ottawa. K1A 0G1.

copper values that led to the subsequent discovery of the potential open-pit deposit.

The property was examined and drill cores sampled and logged by the writer in the summer of 1973. The principal purposes of the examination were to determine whether the deposit is similar to the Babine Lake porphyry copper deposits (Carson and Jambor, 1974) and to see whether hydrothermal biotitization shows a close relationship to the copper zone.



GSC

Acknowledgments

This study could not have been undertaken without the generous cooperation of the staff of Bethlehem Copper Corporation, Ltd., particularly R. Anderson, J. Anderson, and P. Tsaparas, who provided access to the Maggie drill core and information about the property. Discussions with D. Miller of Bethlehem were of considerable assistance and are gratefully acknowledged. The writer's indebtedness to A.G. Plant and G.J. Pringle of the Geological Survey for the many microprobe analyses is readily apparent. Support at the Geological Survey was also kindly provided by numerous staff members, especially R.N. Delabio, J. Kempt, A.C. Roberts, G.R. Lachance, and A. Whitehead. Personnel in CANMET kindly prepared the polished sections used in this study.

GENERAL GEOLOGY

Upper Paleozoic sedimentary and volcanic rocks of the Cache Creek Group (Duffell and McTaggart, 1951) occupy most of the outcrop area around the Maggie deposit (Fig. 2). Dark grey to black chert and argillite is intercalated with green andesite, minor basalt, and abundant agglomerate and tuff. Marble is present in a few outcrops in the northern part of the property. The largest outcrop of volcanics in the southwestern part of the map-area (Fig. 2) differs from other parts of the Cache Creek Group and consists of pumpellyite-bearing porphyry and breccia with associated ignimbrite, possibly indicating proximity to a volcanic centre.

The Cache Creek Group has been complexly folded and intruded by numerous plugs and sheets of serpentinized ultramafic rocks. Bedding attitudes are highly variable, but the predominant strike seems to be northwesterly; most dips are moderate to steep.

The Maggie copper deposit is centred in a series of early Tertiary¹ dyke-like salic porphyritic intrusions, most of which have a northerly strike and steep westerly dip. Nearly all of the copper-bearing porphyries underlie the valley of Bonaparte River and are covered by considerable thicknesses of overburden. However numerous dykes and small irregularly shaped intrusions, which outcrop in the peripheral areas, are similar to some of the porphyries intersected in drillholes; correlation suggests that most of the outcrops represent the intrusive phases that lie along both the footwall and hanging wall of the main copper-bearing porphyry.

The youngest bedrock in the area consists of unaltered and unmetamorphosed volcanic and sedimentary rocks which probably are part of the Eocene-Oligocene Kamloops Group. These post-date the Maggie porphyries. The volcanics are dark brown to black andesitic and

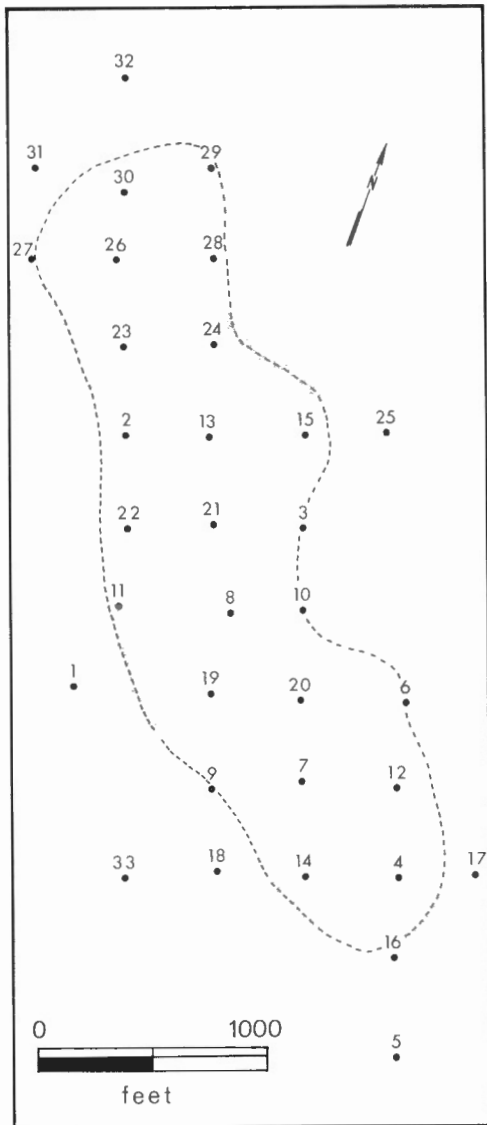


Figure 3. Location of the diamond-drill holes bored by Bethlehem Copper at the Maggie property. The dashed line, shown also on Figure 2, encloses the area with >0.2% Cu as estimated from megascopic sulphides and from the microscopically-determined distribution and quality of hydrothermal biotite.

Figure 2 (opposite)

Geology of the Maggie property, based essentially on the unpublished work of Miller (1972), but with some modifications. Outline of the pyrite halo and the position of the 0.2% Cu zone are from this study. Relative ages of the lithological subdivisions of the Cache Creek Group are not known. Unit 6 (Tertiary) is correlative, at least in part, with the quartz monzonite porphyry which is the principal host rock of the overburden-covered copper zone.

¹McMillan (1970) reported a K-Ar age of 61.1 ± 2 m. y. for a sample of Maggie hydrothermal biotite. The sample was from D. D. H. MM-16 (McMillan, pers. comm., 1975), which suggests that the rock dated was biotitized volcanic material belonging to the Cache Creek Group.

basaltic flows, commonly vesicular to amygdaloidal, and breccias. Red to brown sandstone, grit, and conglomerate of local derivation are intercalated with the volcanics.

Near the Maggie property, the unaltered rocks of the Kamloops Group form the eastern hillside along Bonaparte River valley. Miller (1972) showed the Cache Creek and Kamloops groups separated, for the most part, by a north-striking fault approximately three miles long that parallels Highway 97. The position of the fault at about 6000 feet southeast of the copper zone was indicated by D.D.H. MM-34 (Fig. 2), drilled at -45°E . After passing through overburden, the hole intersected more than 700 feet of Kamloops Group rocks.

PORPHYRY INTRUSIONS

Porphyritic diorite and quartz diorite

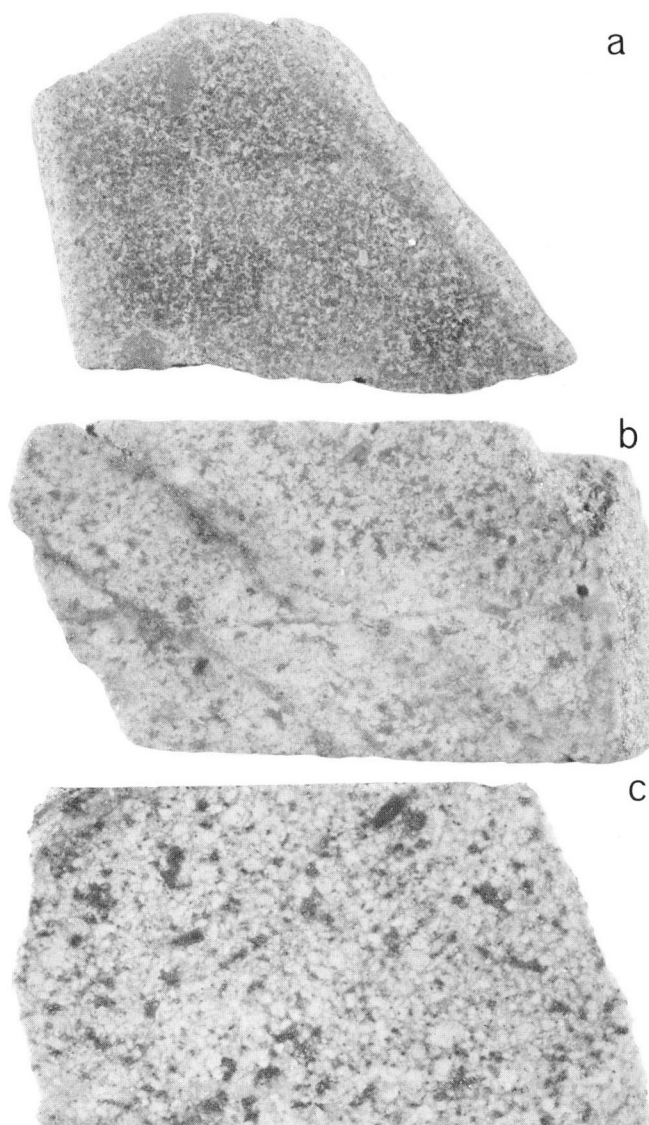
The oldest of the Maggie intrusions consist of porphyritic diorite and quartz diorite. They are exposed west of the copper zone (Fig. 2), and were intersected principally in diamond-drill holes MM-1, MM-30, and MM-32 (Fig. 3). Although minor dioritic dykes occur in the copper zone, most of these intrusions are in the pyrite halo along the hanging wall of the Cu zone (Fig. 2).

The megascopic appearances of the diorite and quartz diorite are shown in Figure 4. Characteristic features are the relatively coarse matrix and more subdued porphyritic texture in comparison with those of the younger intrusions. Microscopically, the dioritic rocks consist largely of oscillatory-zoned plagioclase phenocrysts in a fine grained matrix of zoned plagioclase with variable interstitial quartz. Phenocryst sizes range from 2 to 8 mm, whereas most matrix feldspars are 0.2 to 0.8 mm in length. Cores of phenocrysts are as calcic as An_{60} ; rims are considerably more sodic and are compositionally overlapped by matrix plagioclases which average An_{35-25} , and range from An_{45} to An_{15} .

Dioritic rocks near the Maggie copper zone have been affected drastically by hydrothermal alteration, including intense pyritization. Biotite phenocrysts generally persist in all but the most severely sericitized parts of the porphyry. In contrast, significant amounts of amphibole in porphyry are present only beyond the outer limits of abundant copper. Such amphibole occurs as disseminated crystals, commonly euhedral, that average about 0.3 mm in basal section and make up about 7 per cent of the rock. Slightly larger biotite phenocrysts and disseminated magnetite average about 2 per cent.

Although the dioritic intrusive phase near the copper zone is also referred to as quartz diorite (Figs. 2, 6), the latter name is a generalization applicable only to the bulk of the porphyry along the hanging wall. In addition to multiphase intrusion evident in outcrops¹,

¹Seen best in outcrops about 6000 feet west of Veasy Lake, beyond the map-area.



(a) hand specimen of diorite from near the outer limits of the pyrite halo, west of the copper zone;
 (b) D.D.H. MM-33, showing sericitized quartz diorite;
 (c) 150 feet deeper in same hole, showing more clearly the porphyritic texture, coarser than in (a). All photos full-size reproductions.

Figure 4. Diorite and quartz diorite from Maggie deposit.

thin section studies of the hanging wall porphyry indicate that it is variable in composition. For example, the primary composition (i.e. excluding alteration phenomena) of the quartz diorite at the northwestern end of the copper zone (D.D.H. MM-32) is less calcic than the quartz diorite in D.D.H. MM-1. Even more significant is the fact that the porphyritic masses exposed west of

Table 1

Chemical analyses of diorite and quartz monzonite porphyry intrusions, Maggie deposit

	(1)	(2)	(3)	(4)	(5)	(6)	(7)	(8)
Wt. %	M74-1	M74-17	19-217	19-374	19-448	19-1289	19-2001	19-2079
SiO ₂	59.3	57.	64.	66.	66.	62.	66.	66.
TiO ₂	0.92	0.98	0.60	0.64	0.59	0.85	0.59	0.54
Al ₂ O ₃	17.1	17.5	17.	16.	17.5	19.	18.	18.
Fe ₂ O ₃ *	5.86	6.6	3.8	4.7	1.7	3.1	1.7	1.8
MnO	0.13	0.11	0.03	0.03	0.02	0.02	0.01	0.01
MgO	2.78	3.6	1.8	1.7	2.2	2.2	1.8	1.7
CaO	5.38	6.4	2.8	3.0	2.6	1.8	1.9	2.1
Na ₂ O	4.6	4.1	4.1	4.4	4.9	3.5	4.6	4.2
K ₂ O	2.18	2.3	2.4	2.0	2.3	2.8	4.1	4.0
P ₂ O ₅	0.36	0.45	0.27	0.30	0.28	0.35	0.30	0.28
CO ₂	0.3	0.3	0.38	0.02	0.23	0.13	0.34	0.05
H ₂ O	1.5	1.5	1.6	1.3	2.0	3.5	1.5	1.5
S	0.04	0.31	1.7	0.59	0.52	1.0	0.61	0.60
Total	100.1	100.8	100.5	100.9	100.8	100.5	101.4	101.1

Analyses by Rapid Methods Group, CLAS Division, Geological Survey of Canada

*Total Fe as Fe₂O₃

- (1) Diorite porphyry, west of Veasy Lake (Fig. 5a).
- (2) Diorite porphyry from outer edge of pyrite halo (Fig. 4a).
- (3) Finer grained phase of quartz monzonite porphyry in D.D.H. MM-19 at 217 feet (see Figs. 7b, c and Fig. 10). Sample contains 0.41% Cu. The rock is a porphyritic granodiorite in the biotite zone of hydrothermal alteration.
- (4) D.D.H. MM-19 at 374 feet, similar to (3) above, with 0.27% Cu.
- (5) Similar, with 0.18% Cu. Matrix plagioclase compositions, An₉₋₁₅, shown as third from top of D.D.H. MM-19 on right-hand side of Figure 10.
- (6) D.D.H. MM-19 at 1289 feet, the position marking the change from megascopic unit 2 to "normal" unit 3 (Fig. 10, left). Sample contains 0.40% Cu.
- (7), (8) Unit 3 of Figure 10. The samples contain 0.35 and 0.45% Cu respectively.

Samples (3) to (8), inclusive, are from the biotite zone of hydrothermal alteration.

the drillhole area are, at least for the most part, diorites rather than quartz diorites. The diorites have substantially less interstitial quartz, and matrix plagioclases are more calcic than those in the quartz diorite.

Quartz monzonite porphyry

The overburden-covered Cu-Mo zone is contained in a complex, multiphase, porphyritic intrusion that is designated simplistically as "quartz monzonite porphyry". Although quartz monzonite porphyry, *sensu stricto*, does constitute an important part of the intrusion, an estimated one half to two thirds of the volume of the copper-bearing porphyry consists of

granodiorite, and insignificantly minor parts have the composition of granite; nevertheless, quartz monzonite was selected as the general term in order to draw attention to the widespread occurrence of abundant K-feldspar phenocrysts.

The quartz monzonite porphyry forms a highly irregular, somewhat tabular body that dips westward and, at bedrock surface, is elongated to the northwest. Extensive interfingering of the porphyry with host ultramafic rocks and the Cache Creek Group occurs not only along the flanks of the intrusion, but also at the northwestern end of the copper zone. Drillhole data suggest that the porphyry pinches out towards the

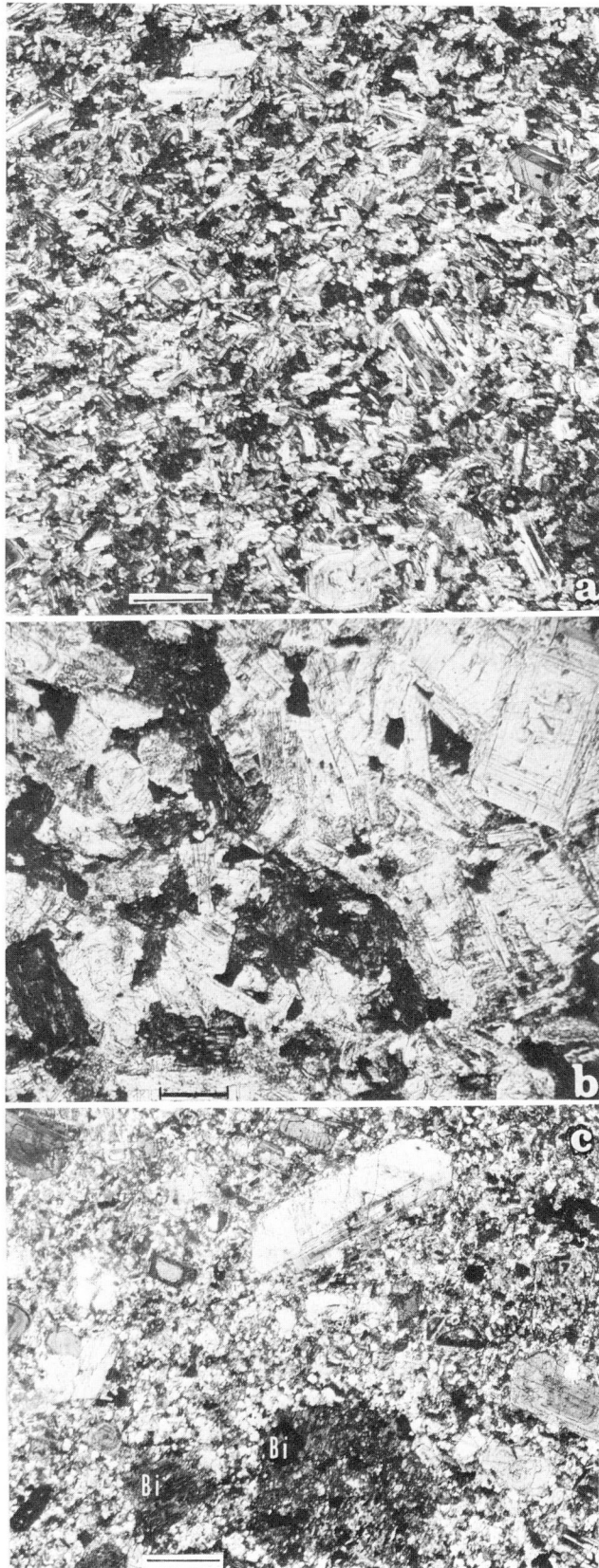


Figure 5. Photomicrographs of:

- (a) unaltered diorite, approximately 6000 feet west of Veasy Lake (bar scale: 2mm);
- (b) enlargement showing well-defined, zoned plagioclase and relatively unaltered, darker amphibole (bar scale: 0.1mm);
- (c) quartz diorite from D. D. H. MM-1 at 1873 feet; well-zoned plagioclase phenocrysts in a biotitized finer matrix. Biotite phenocrysts (Bi) are finely rutiled and sericitized (bar scale: 2mm).

north, but equivalent information is lacking south of the copper zone (west of D. D. H. MM-5, Fig. 3).

The longest and most complete drill intersection of quartz monzonite porphyry is in D. D. H. 19, which penetrated more than 2200 feet of the intrusion and may have reached its bottom contact (Fig. 10). Of the various drill-intersected phases of the porphyry (Figs. 6, 10), only the finest grained variety outcrops as minor dykes in the hills that border the copper zone. However, a closely related breccia, grouped with the quartz monzonite porphyry in this paper, is well-exposed adjacent to Highway 97, southeast of the nearby copper zone. The breccia was also intersected in drill-holes in the southeastern part of the deposit.

Although the quartz monzonite porphyry is younger than the diorite and quartz diorite porphyry, all are believed to be closely related and representative of a single intrusive episode.

Megascopic subdivisions of the quartz monzonite porphyry intrusion

All quartz monzonite porphyry at the Maggie property has been modified by hydrothermal alteration. Rocks that appear least altered megascopically generally occur in the highest grade parts of the copper zone, a situation analogous to that found by Carson and Jambor (1974) in the porphyry copper deposits of the Babine Lake area of British Columbia. The apparently less altered appearance of the rocks is attributable to the general lack of significant feldspar-destructive alteration within the highest grade portions of the copper zones.

The most distinctive megascopic feature of the Maggie quartz monzonite porphyry is the presence of abundant, large plagioclase phenocrysts in a fine grained matrix. The phenocrysts are more numerous and coarser, and the matrix finer, than those in diorite-quartz diorite (Figs. 4, 7). Biotite phenocrysts make up 2-4 per cent of the quartz monzonite; the crystals range from <1 mm to >5 mm in basal diameter, with grains 2-3 mm in diameter being most common. Representative chemical analyses (Table 1) indicate that all varieties of the quartz monzonite porphyry have higher SiO₂, and lower CaO, MgO, Fe, MnO, and TiO₂ than the diorite porphyry.

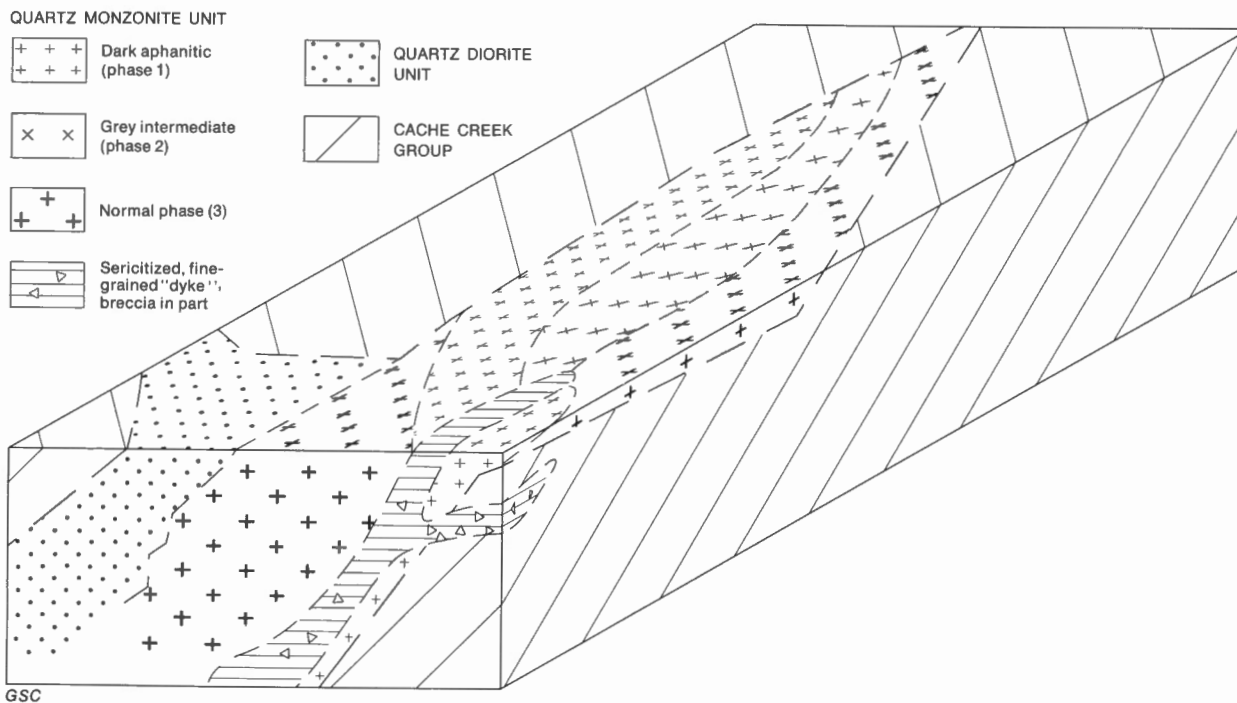


Figure 6. Schematic diagram (looking northwest) showing the relationships of the various Tertiary porphyries that intrude the Cache Creek Group and younger ultramafic bodies (not separated in the diagram). The oldest Tertiary porphyritic unit, diorite-quartz diorite, was intersected in a few drillholes and outcrops west of the copper zone (Fig. 2). The principal porphyritic intrusion, with which the Cu-Mo is associated, was subdivided megascopically into three main varieties: (1) dark, aphanitic matrix, (2) medium grey, coarser grained, (3) "normal" phase, possibly coarser than (2) and lighter grey. The predominantly-sericitized, dyke-like unit is considered to be a variant of phase (1). The numbered varieties of porphyry range in composition from granodioritic to granitic, and are referred to collectively in this paper as quartz monzonite porphyry.

During logging of the core by the writer, an attempt was made to subdivide the quartz monzonite porphyry into three units as follows:

- (1) black to brownish black colour, matrix aphanitic;
- (2) medium grey, mafic-rich, not as fine grained and with more abundant feldspar phenocrysts than above;
- (3) a "normal" phase, lighter grey and possibly coarser than unit (2), matrix less mafic-rich.

The poor condition of some of the core, the presence and variability of intense hydrothermal alteration, and especially the lack of adequately definitive criteria made the distinction between units (2) and (3) difficult in many cases. The apparently gradational contacts between the units did not ease this difficulty. Nevertheless, subsequent plotting of the logs gave a systematic pattern in that the aphanitic unit (1) consistently appeared along the hanging wall part of the intrusion, the medium grey, less fine grained unit (2) formed most of the core of the intrusion, and the "normal" unit (3) was concentrated at the northern and southern ends and along the deepest central part of the footwall. A schematic diagram illustrating the distribution of the

megascopically distinguished phases of the intrusion is given in Figure 6.

Microscopic subdivisions of the quartz monzonite porphyry intrusion

In addition to the megascopic features mentioned previously and shown in Figures 7 and 8, microscopic examination shows that the feldspar phenocrysts consist predominantly of subhedral oscillatory-zoned plagioclase, some with perthitic rims. Slightly smaller, anhedral perthite phenocrysts are common; these exceed plagioclase only locally, the proportions of the two being dependent, in part, on the position of a sample within the intrusion. Quartz phenocrysts, averaging about 2 mm in diameter, make up about 2 per cent of the porphyry. Several per cent sucrose hydrothermal biotite occurring as poorly defined pseudomorphs after amphibole phenocrysts is present in places (Fig. 9), but the abundance and size of the original amphibole crystals are not determined readily because their outlines are not well-preserved.

Attempts to correlate the writer's megascopic logging with features observed microscopically proved perplexing as little correlation was evident in several

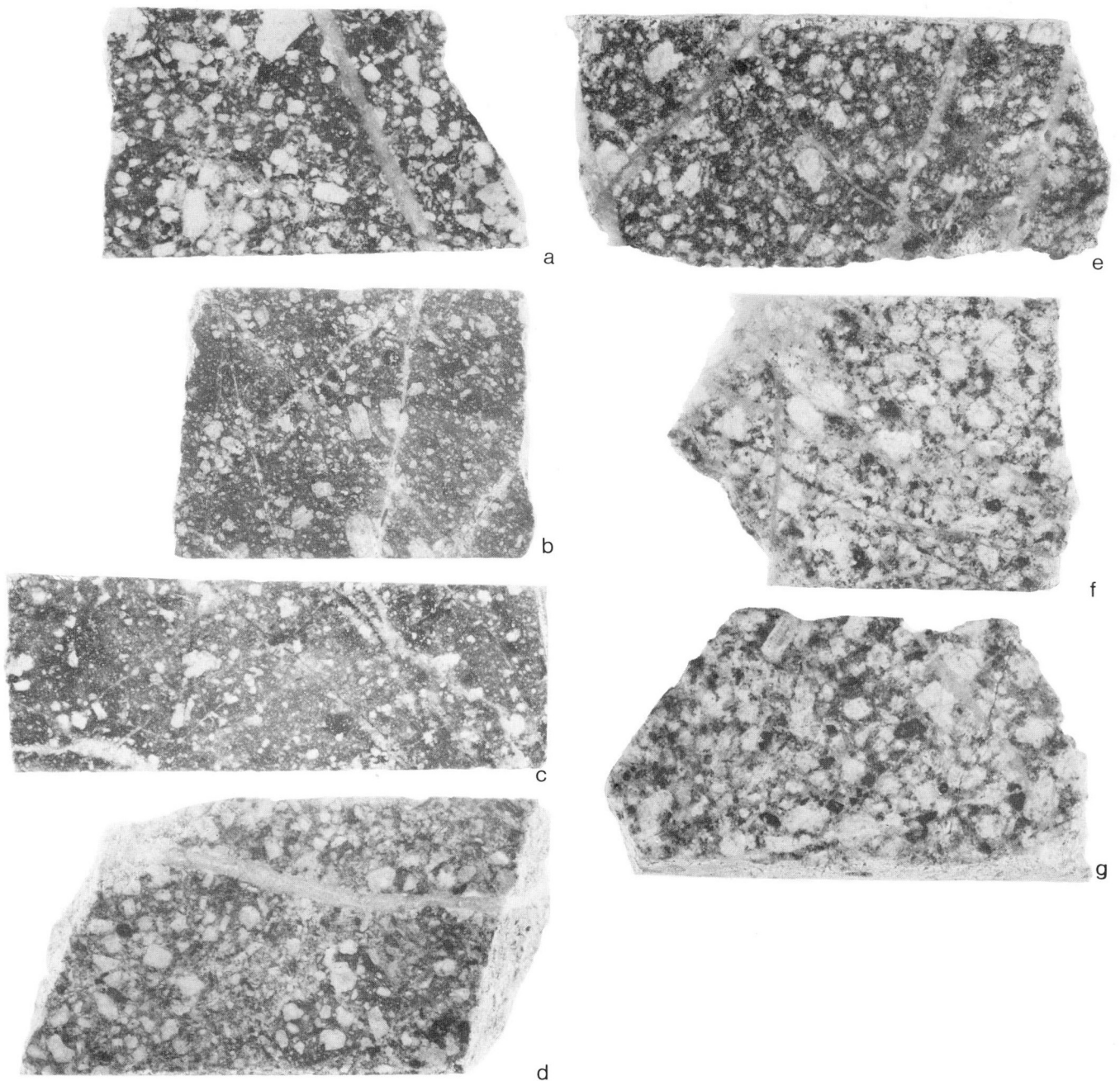
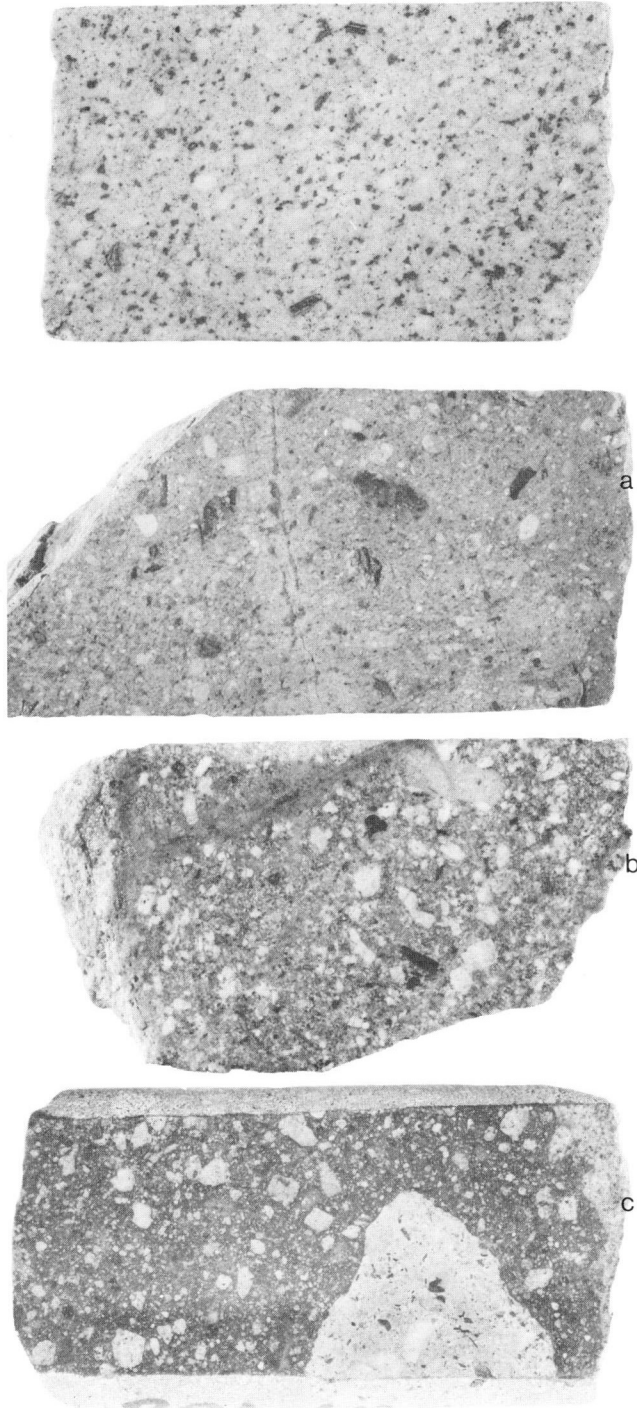


Figure 7. Drill core showing the variability in the megascopic appearance of the quartz monzonite porphyry:

- (a) fine grained unit with aphanitic matrix, D. D. H. MM-3 at 437 feet;
- (b) fine grained unit in D. D. H. MM-19 at 326 feet;
- (c) fine grained unit in D. D. H. MM-19 at 685 feet;
- (d) intermediate, medium grey unit (2) of the megascopic subdivisions, from D. D. H. MM-10 at 465 feet;
- (e) intermediate unit in D. D. H. MM-19 at 867 feet;
- (f) megascopically "normal" unit (3) in D. D. H. MM-19 at 1468 feet; and
- (g) at 2079 feet.

All rocks are from the biotite zone of hydrothermal alteration (natural scale).

Figure 8 (left). Maggie deposit drill cores:



- (a) fine grained, light coloured phase that forms most of the dyke-like unit shown in Figure 6. The "dyke", about 200 feet wide, has abundant associated breccia (see Fig. 8b). The specimen contains large albite phenocrysts and abundant non-perthitic K-feldspar. Dark "mafics" are replaced completely by sericite, carbonate, and pyrite. D.D.H. MM-12 at 327 feet;
- (b) breccia in MM-12 at 462 feet, showing abundant rock fragments of various sizes and shapes;
- (c) breccia from MM-4 at 796 feet;
- (d) breccia with very finely biotitized matrix containing inclusions of chlorite-altered, fine grained quartz monzonite porphyry; D.D.H. MM-17 at 917 feet (natural scale).

cases. Measurements of matrix grain sizes indicated great variability over not only the length of a drillhole, but also among the adjoining samples. Figure 10 illustrates a case where megascopic and microscopic correlation is fair, and Figure 11 illustrates an example in which the correlation obtained was very poor. In the latter, most of D.D.H. 8 and 10 were logged as unit (1) and unit (2) respectively. Grain size variability is especially evident in D.D.H. 10, and in both holes rock compositions vary from granodiorite to quartz monzonite, the exception being the central part of D.D.H. 8, which is porphyritic granite. No specific feature accounts for the poor correlation between megascopic and microscopic rock types; the textural and compositional variability of the rocks is clearly more complex than indicated in the logging.

The occurrence of porphyry of granitic composition in D.D.H. 8 is not anomalous; throughout most of the intersected length of the intrusion are relatively narrow sections in which perthitic phenocrysts exceed those of plagioclase (single crystals of K-feldspar are present also, but are uncommon). The matrices of such rocks are correspondingly K-rich, and the subordinate accompanying plagioclase (<1/3 total feldspar) are generally albite.

Near bedrock surface, albitic and K-rich parts have an approximately medial distribution along the strike of the thicker and less fine grained portions of the intrusion. Westerly, down-dip continuation is evident in some drillholes, but is either absent or more complicated in others.

Finer grained quartz monzonite porphyry and associated breccias

d

The finer grained phase of the quartz monzonite intrusion is characterized principally by having matrix grain sizes that average less than 0.04 mm (Figs. 10, 12). Based on thin section studies, the distribution of the phase in drillholes is shown in Figure 13. Though not restricted to the southeastern half of the intrusion,

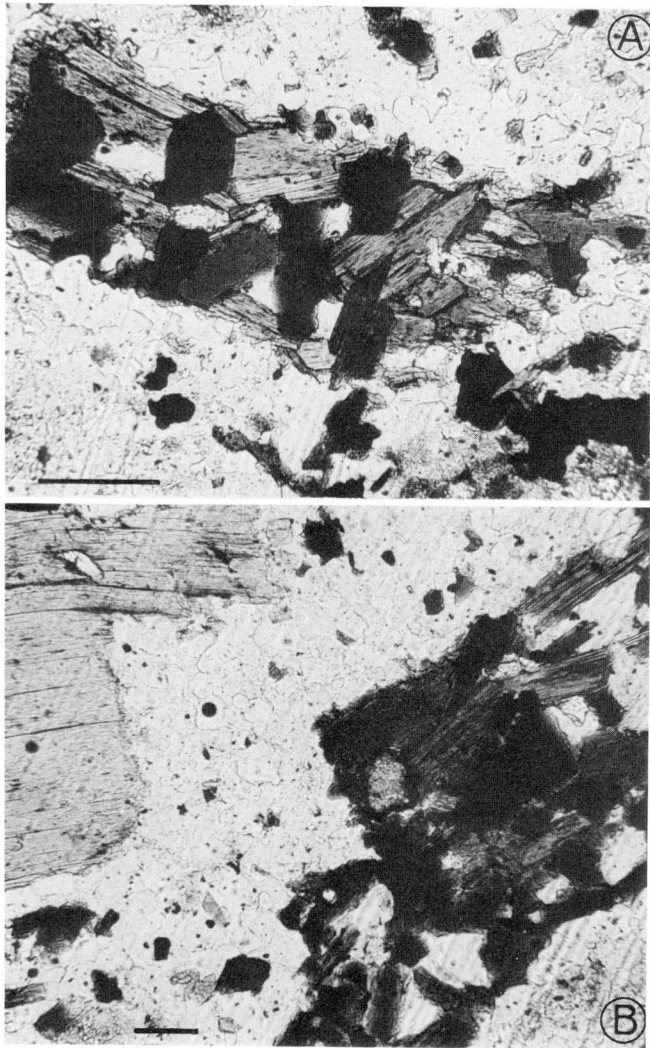


Figure 9. Hydrothermal biotite in D. D. H. MM-6 at 371 feet: (A) coarse sucrose pseudomorph after amphibole phenocryst; (B) probable pseudomorph as above, but with outlines less well-preserved; unaltered biotite phenocryst is at left. Bar scales 0.2 and 0.1 mm respectively.

occurrences of this rock type are clearly concentrated in this area. Figures 10 and 14 show the distribution of the phase in cross-sections.

Compositional variability of the finer grained rocks is as great as that of the coarser grained portions of the intrusion. In addition, however, much of the finer grained phase at the southeastern part of the deposit contains albite to an extent not seen elsewhere, and much of the rock is breccia.

The breccia is not easily characterized megascopically and unless abundant rock fragments are present, the breccia looks very much like the more extensive, non-brecciated, finest grained unit of the quartz monzonite porphyry, such as occurs in the top of D. D. H. 19 (Figs. 7, 12). Microscopically, both

rock types contain large feldspar and smaller quartz phenocrysts with corroded margins. However, in breccia, phenocrysts are commonly fractured or only fragments, strongly zoned calcic plagioclase is much less abundant than poorly zoned albitic feldspar, large unzoned albite grains are common, perthite is rare, and diverse subrounded rock fragments occur in an extremely fine groundmass that in some cases has grain sizes <0.01 mm.

The breccia is well exposed on the eastern side of Highway 97 at the southeastern end of the Maggie deposit, and was intersected principally in D. D. H. 12 and 17. In these occurrences complex age relationships are evident, but most of the breccia seems to be a younger phase closely related to the quartz monzonite porphyry. This close temporal relationship is indicated by the fact that all breccia is pyritized and hydrothermally altered. The inter-mineral (Kirkham, 1971) character of the breccia is evident from the presence of inclusions of quartz-veined, coarser grained quartz monzonite porphyry, and the presence of non-biotitized fragments of breccia enclosed in younger breccia having an extremely finely biotitized matrix.

The above relationships indicate that intrusion and brecciation did not cease completely prior to sulphide deposition and hydrothermal alteration. The intimate associations and gradational character of many of the porphyries, apparent from both compositional and textural features, also suggest that all rocks, from diorite to quartz diorite to quartz monzonite and fine grained phases and breccias, are closely related and are part of a single intrusive episode.

SULPHIDE MINERALIZATION

Pyrite

Intense pyritization is a distinctive feature at the Maggie deposit. Much of the prominent gossan surrounding the deposit is the weathered residue of rocks that contained 5 to 10 per cent pyrite by volume. The mineral occurs both as disseminated grains and along fractures in all rock types, but ultramafics seem to have been the least susceptible to impregnation. Volcanics and the porphyritic intrusions were the most favourable hosts, and in some cases the volcanics, along several feet of drill core, consist mainly of sulphides, principally pyrite. Although pyrite is most abundant in the gossan area, it occurs in lesser amounts throughout the copper zone. The hanging wall of the deposit seems to have been the most intensely pyritized, and the northeastern part of the copper zone the least pyritized. Pyrite abundances change vertically as well as horizontally so that a more detailed study would be necessary to establish whether, within the core of the halo, centres of minimal pyrite are present. Logging by the writer suggests that there is a trend to relatively lower pyrite abundances in D. D. H. 28, 24, and 13 (Fig. 15), but this does not continue without interruption into the southern half of the deposit. Thus both the petrology and pyritization seem to differ in the northern and southern parts of the deposit; overall, the southern

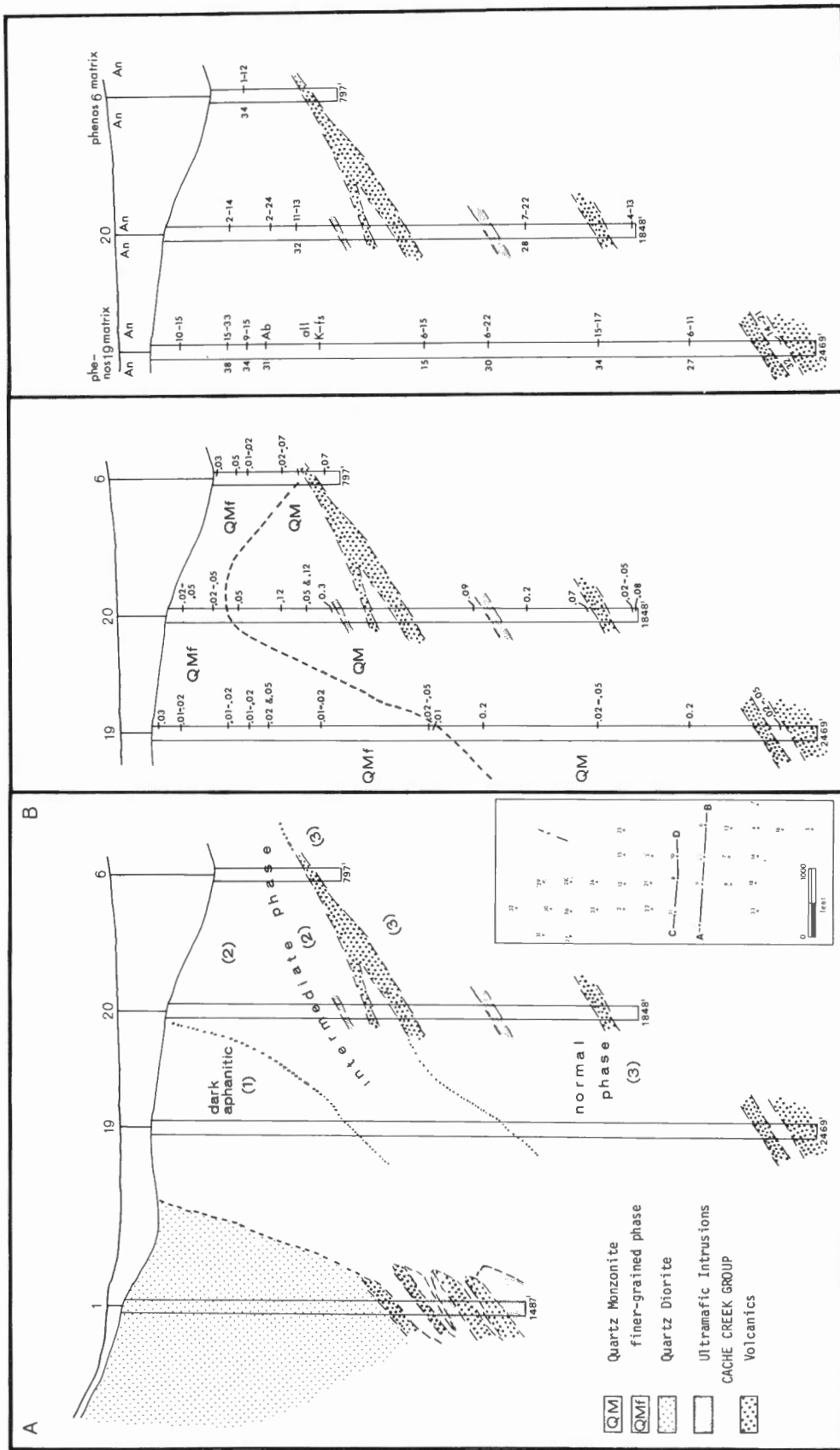


Figure 10. Comparison of subdivisions of the quartz monzonite porphyry as determined by megascopic logging (left), and by microscopy (centre). The central diagram also shows average grain sizes, in mm, of the matrices as measured in thin sections. Diagram to the right shows average compositions of plagioclase phenocrysts, and ranges of compositions (wt. % An) of matrix plagioclases, as determined by microprobe analyses. Section C-D of inset is shown in Figure 11.

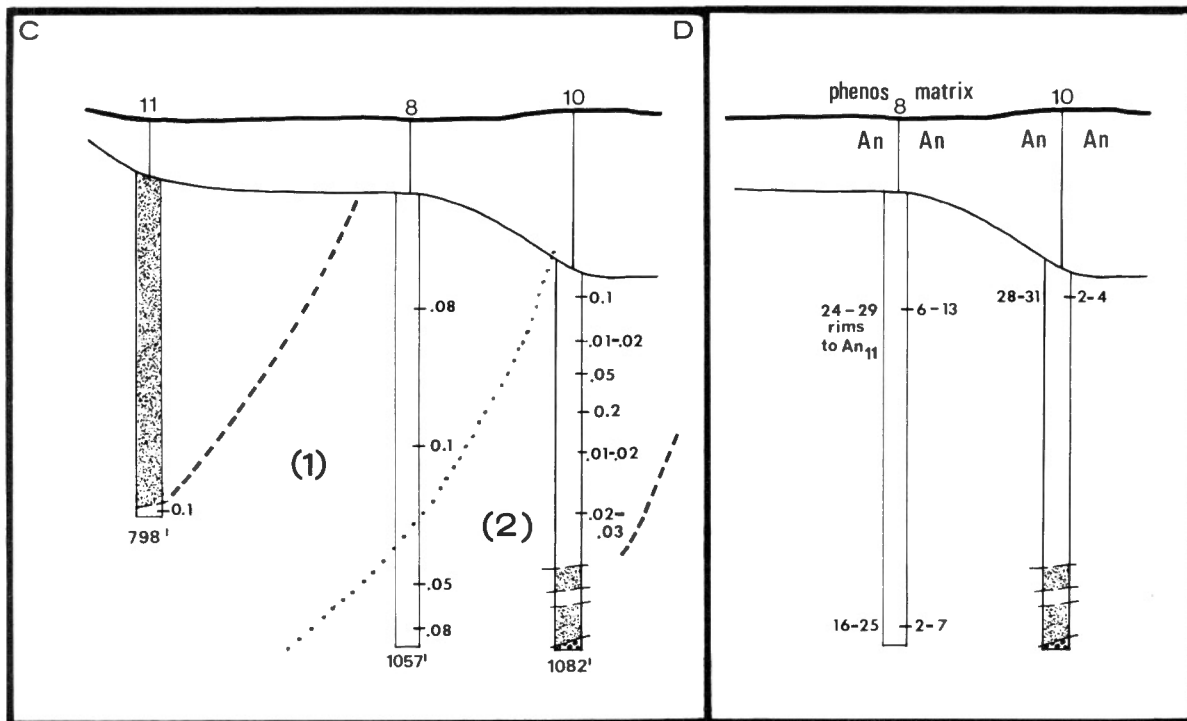


Figure 11. Cross-section C-D (inset in left part of Fig. 10), illustrating an example of poor correlation between the megascopic and microscopic results: the top three quarters of hole 8 were logged megascopically as phase (1), and the bottom one quarter and hole 10 were logged as phase (2). Variability in matrix grain sizes is evident especially in D.D.H. 10. Phenocryst compositions, and matrix grain sizes and compositions, were determined as for Figure 10. Stippled unit is chert and argillite of Cache Creek Group, but otherwise the legend and scale are as in Figure 10.

part has a much larger volume of porphyry and is more intensely pyritized.

The surface occurrence of the pyrite halo is shown in Figure 2. In outcrops west of the copper zone, pyrite abundances decline westward in a regular manner. Northwest of the copper zone, in the large fault-displaced segment of the halo, pyritization is much less uniform; occurrences are sporadic and abundances are variable from outcrop to outcrop. However, near the Maggie adit, pyritization stops abruptly.

Although the pyrite halo is shown (Fig. 2) as a continuous zone elongated northwesterly, this continuity is achieved by projection across the Bonaparte River valley, which is devoid of outcrops. If the projection were not made the pyrite halo could be shown in Figure 2 as two segments, divided by Highway 97, with the eastern segment displaced southward. However, the available geological information precludes the occurrence of the major north-striking fault, or faults, which would be necessary to restore the two segments to a single, originally more elliptical halo.

Ore minerals

Chalcopyrite is the only widespread, abundant copper mineral. It occurs in all rock types as minute disseminated grains, and as megascopic and microscopic veinlets, generally with quartz. In the copper zone, the proportion of chalcopyrite that occurs in disseminated

form is very high; an estimated one third of the volume of the mineral is present as grains unrelated to veinlets, even on a microscopic scale.

The relatively low abundance of bornite at the Maggie deposit is indicated by the fact that the mineral was not observed by the writer during logging of the drill core, and was found associated with chalcopyrite only in polished sections of material from the central part of the copper zone.

Molybdenum is confined largely within the copper zone. Some occurs as fine grains (0.01-0.05 mm) and aggregates (0.05-0.2 mm) disseminated in the ground-mass of the quartz monzonite porphyry, but most is conspicuously visible in quartz veinlets, many of which contain drusy quartz coated with well-crystallized molybdenite flakes up to 1 mm in diameter.

Tennantite was found in veinlets, 2-4 mm wide, in five drillholes. In one sample (M-31 at 562 feet) the mineral occurs with quartz and white, pulverulent barite; in another (M-30 at 801 feet) galena and sphalerite are associated. Unit-cell sizes of the tennantites are mostly those of the arsenic end-member, but in at least one sample, the mineral had a significantly larger cell. Whether the enlargement is caused by antimony, silver, or some other substitution has not been investigated.

The distribution of observed tennantite occurrences is shown in Figure 16. Though the occurrences are few, their concentration near the periphery of the copper zone is notable.

Table 2
 Characterization of hydrothermal biotites in terms of quality.*

	Good Quality	Moderate Quality	Poor Quality
Colour in thin section	deep brown	brown	pale brown to yellowish, pale red, greenish brown to green
Relative grain sizes	coarse	medium	fine
Pseudomorphism of mafics	coarse grained, sugary-textured	medium to coarse, sugary-textured	fine grained, commonly with intimately associated fine grained chlorite
Presence in matrix	well-dispersed in matrix	generally absent	absent
Distribution in thin section	abundant: all amphibole replaced; dispersed in matrix	abundant; all amphibole replaced, but matrix biotite low or absent	variable; if abundant, most of the above features are present
Effect on biotite phenocrysts	no effect to replacement of phenocryst edges	no effect	no effect
Synonyms	intense biotitization; strong biotitization	moderately intense biotitization	weak biotitization
Areal abundance and general relationship to Cu grades	present throughout the >0.3% Cu zones in most Babine-type deposits	common within 0.2%-0.4% Cu zones	rare in zones containing >0.3% Cu; common where Cu = 0.1%-0.2%; where Cu <0.15% nearly all biotite is of this type

*After Carson and Jambor (1974), with slight modification.

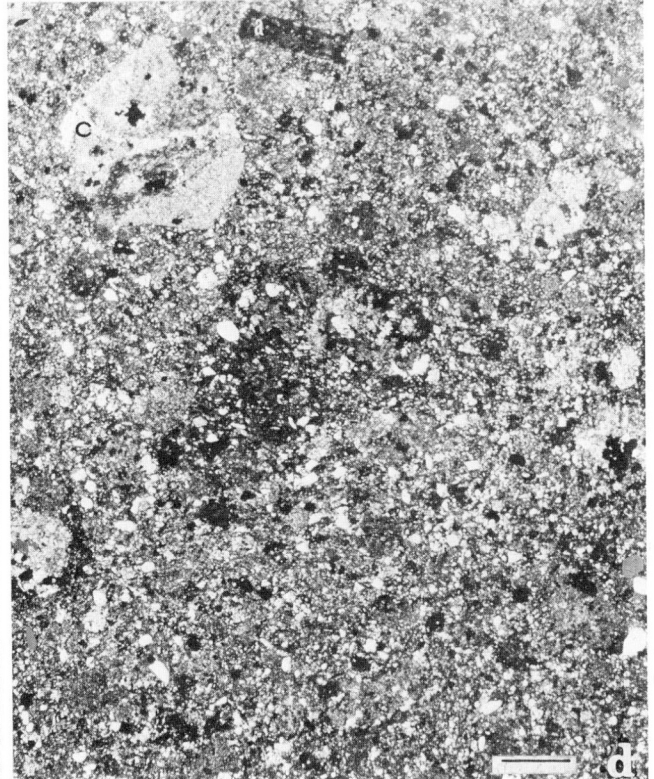
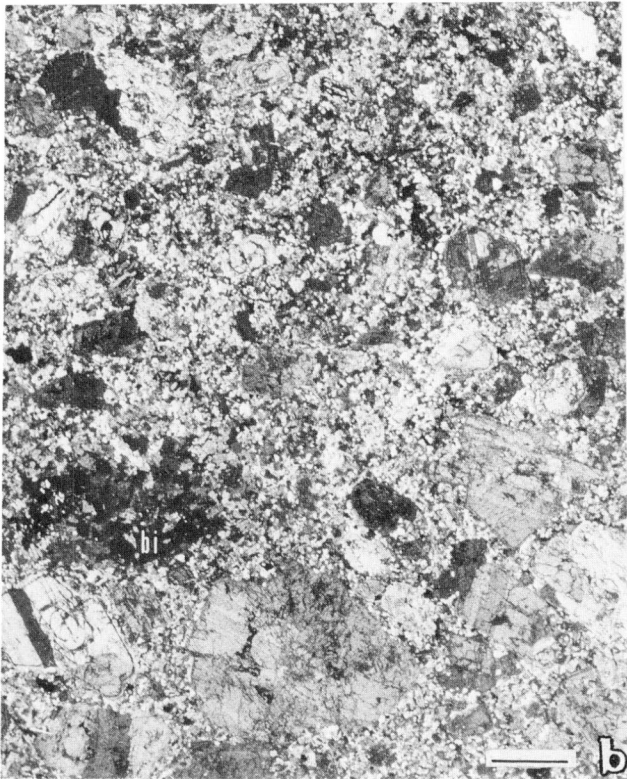
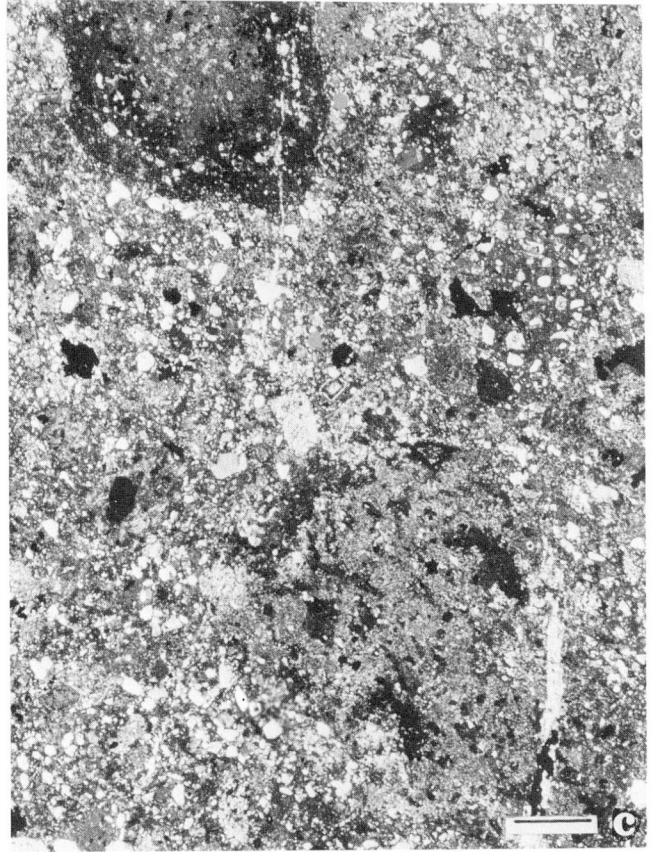
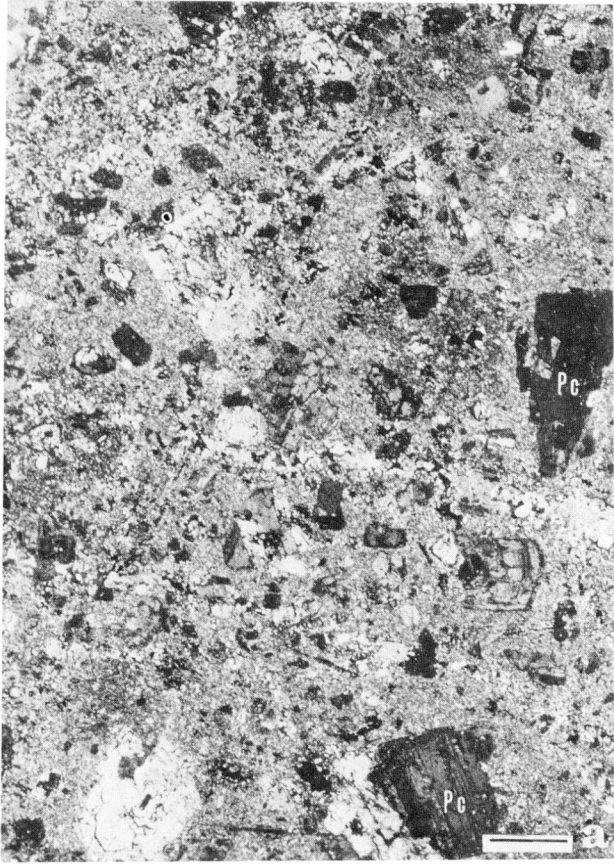
Traces of chalcocite and covellite have been noted in samples from the copper zone, and microscopic aggregates of marcasite are present both in the copper zone and pyrite halo. The occurrence of these minerals near the bottoms of some holes suggests a hypogene origin. Pyrrhotite is common as microscopic blebs in pyrite throughout the copper zone and pyrite halo. Sphalerite has been noted in microscopic veinlets in D. D. H. MM-13 and MM-30.

The distributions of pyrite and copper sulphide minerals as outlined above suggest that the sulphide zoning at the Maggie deposit conforms to the "ideal" outward progression of bornite→chalcopyrite→pyrite. That the conformity is developed only primitively is reflected in the lack of a well developed bornite zone, and the lack of a definable chalcopyrite-pyrite boundary inside the copper zone. Although the limits of +0.2% Cu have been estimated visually (Fig. 3), pyrite occurs abundantly throughout all parts of the deposit, and chalcopyrite extends well into the hanging wall pyrite halo. However, less chalcopyrite is present in the

footwall part of the pyrite halo and, as mentioned previously, less pyrite also seems to be present along parts of the eastern margin of the copper zone. Thus the relatively poor segregation of the sulphides may reflect not only the low grade of the deposit, but also distortions arising from the inclined, asymmetrical shape of the porphyritic host intrusions.

HYDROTHERMAL ALTERATION

The Maggie Cu-Mo zone and surrounding rocks have been affected strongly by hydrothermal alteration whose outer limits beyond the pyrite halo are complex and difficult to define precisely. The complexity arises because the geology is incompletely known, because the Cache Creek Group has been metamorphosed, and because porphyritic intrusions are uncommon at the margins of the pyrite halo. The significance of the above is that the metamorphosed rocks contain minerals similar to those produced by weak hydrothermal alteration; thus, propylitic alteration in the Cache Creek rocks is



not readily defined megascopically, and intrusions are too few to be of much help. Although thin section studies of the intrusions have shown that a propylitic assemblage is present in some of the outer parts of the pyrite halo, the effort necessary to separate "altered" and "unaltered" Cache Creek rocks discouraged any serious attempt at defining a propylitic zone. Attention in this study has been focused principally upon biotitization and its relationship to copper mineralization.

Hydrothermal biotitization

The distribution of hydrothermal biotite in drill cores from within a few feet of bedrock surface is shown in Figure 17. The mineral occurs in a variety of rock types, including porphyries and the chert, argillite, and volcanic rocks of the Cache Creek Group. Proximity to the copper zone is an obviously significant relationship.

In the Maggie deposit, which averages about 0.28% Cu, biotitization is similar to that which accompanies 0.2-0.4% Cu at the porphyry deposits in the Babine area, British Columbia (Carson and Jambor, 1974; Table 2, this report). However, some textural differences are evident. In particular in the Maggie deposit pseudomorphs of hydrothermal biotite after amphibole commonly have outlines that are much less well preserved than similar pseudomorphs in Babine deposits; the biotites in the Maggie deposit are not compactly intergrown, but are separated by other silicates, mostly quartz. Thus some hydrothermal biotite grains in poorly preserved pseudomorphs are not distinguished readily from matrix biotites. A further, but minor, complication at the Maggie deposit is that some large, single biotite grains that approach phenocrysts in size have been found to be compositionally similar to hydrothermal biotites. It is not certain whether such

Figure 12 (opposite)

Photomicrographs of phases of the quartz monzonite porphyry:

- (a) fine grained unit in D.D.H. MM-19 at 448 feet; large light and dark plagioclase phenocrysts in a fine matrix with good-quality hydrothermal biotite. Abundant perthite is present along the veinlet at the middle of the photograph;
- (b) biotitized quartz monzonite porphyry, D.D.H. MM-20 at 587 feet. Hydrothermal biotite is present as sucrose pseudomorphs after amphibole (bi, lower left), and is scattered throughout the matrix. Note the coarser grain size of the matrix as compared to that in Figure 12a (both photographs at same magnification; see also Fig. 10);
- (c) breccia in D.D.H. MM-17 at 814 feet;
- (d) breccia from outcrop southeast of copper zone, adjacent to eastern side of Highway 97. Amphibole (a) at top centre is chloritized; adjacent rock fragment (c) is chert, and mottled appearance of matrix is due to inclusions of rock fragments. Most clear grains are quartz, and opaque grains are pyrite. Bar scale for Figure 12 is 2mm.

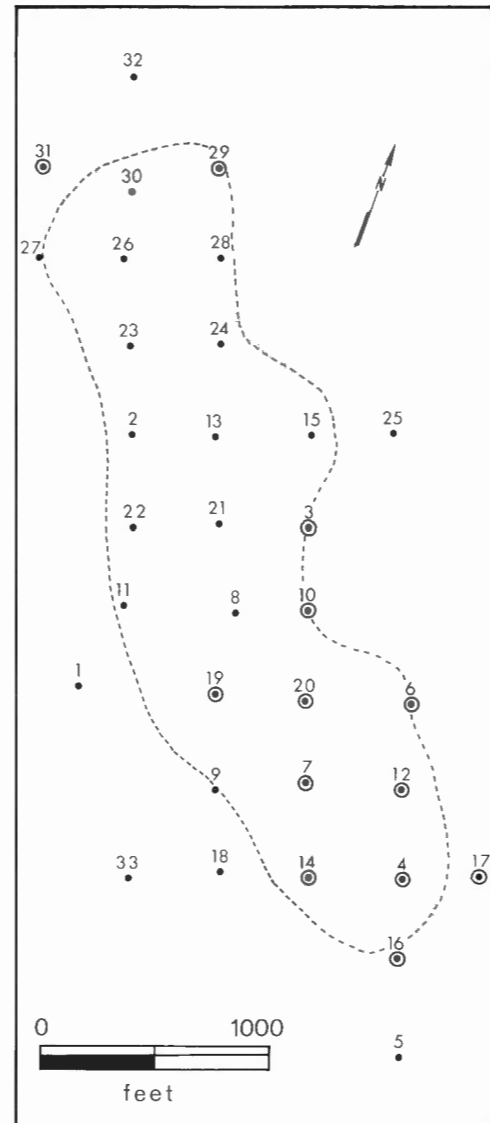


Figure 13. Distribution of the fine grained phase of the quartz monzonite porphyry (open circles) as determined by microscopy. Occurrences are projected vertically to surface.

grains are non-sucrose pseudomorphs after amphibole, or whether they are biotite phenocrysts whose compositions have been modified during hydrothermal alteration.

East-west cross-sections indicate that much of the zone of hydrothermal biotite plunges west. Near the bedrock surface, microscopically dark brown hydrothermal biotite is confined within the estimated +0.2% Cu zone; outside this zone the colour of the mineral is lighter and it exhibits most of the other features characteristic of "poor-quality" biotite as given in Table 2.

Table 3

Comparison of maximum pleochroic colours of biotites and their Fe/Mg+Fe+Mn ratios*

Colour	Sample Numbers	Approximate Fe/Fe+Mg+Mn
very dark brown	M6-449; M8-402, 1031; M13-306, 526, 873	0.40; 0.38, 0.39; 0.33, 0.38, 0.39
moderately dark brown	M19-510, 1082, 1673 (1)	0.25, 0.25, 0.28
medium brown	M19-1673 (3), 2345; M28-548, 895	0.21, 0.18, 0.16, 0.23
pale brown	M1-1183 (1, 2); M28-1219	0.23; 0.16
anomalous brownish green	M24-817 (6)	0.19-0.22
pale green	M24-817 (5)	0.24

*Sample selection based on a scan through a limited number of randomly-selected polished thin sections. Fe/Fe+Mg+Mn values are from microprobe analyses given in Appendix I.

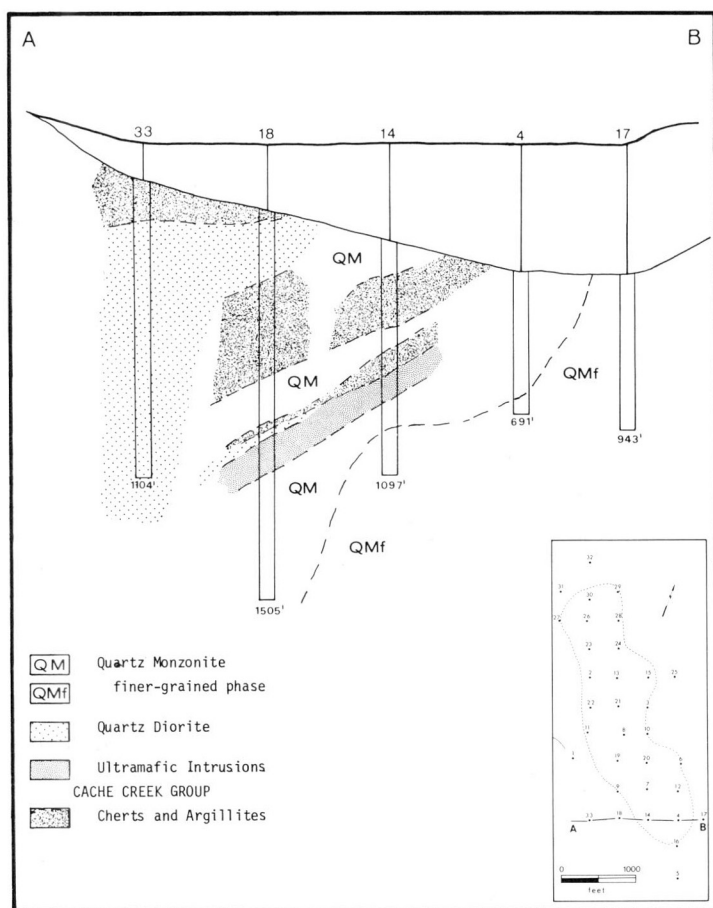


Figure 14. Distribution of the fine grained phase of the quartz monzonite porphyry in cross-section (see also Fig. 10). Much of the phase in holes 17 and 14 consists of breccia (Figs. 8, 12).

Biotite compositions

Electron microprobe analyses of 110 biotites from 10 drillholes (Fig. 18) are given in Appendix I, and a comparison of maximum pleochroic colours in thin sections and Fe/Fe+Mg+Mn atomic proportions is given in Table 3. For the representative samples listed, the trend toward lighter colours as Fe/Fe+Mg+Mn decreases is readily apparent. Noteworthy in Appendix I is the extension of compositions well into the phlogopite field of Deer *et al.* (1962). Thus, some of these trioctahedral micas are not strictly biotites, though they are referred to as such for convenience.

The analyses in Appendix I show that Fe/Fe+Mg+Mn in phenocrysts may be higher or lower than that of the associated hydrothermal biotite. However, titanium is characteristically and distinctively higher in most phenocrysts; this relationship seems to be typical of other porphyry copper deposits for which data are available (Carson and Jambor, 1974; Moore and Czamanske, 1973; Jacobs and Parry, 1974).

The relationship of Ti and Fe/Fe+Mg+Mn is summarized in Figure 19. The plots show that, as mentioned above, Fe/Fe+Mg+Mn in phenocrysts may be higher or lower than that of the associated hydrothermal biotite; the most common trend, however, is for phenocrysts to have more iron than the associated hydrothermal biotites. Of more significance is the observation that the analyses of both the hydrothermal biotites and the phenocrysts in each sample have a distinct tendency to cluster (Fig. 19). For example, those samples with a low Fe/Fe+Mg+Mn ratio in hydrothermal biotite also generally have a low Fe/Fe+Mg+Mn ratio in the associated phenocrysts. As this relationship would not be expected unless the phenocrysts underwent compositional adjustments during hydrothermal alteration, it is concluded that such adjustment has occurred.

Reference to Table 3 shows that the intensity of colour of brown hydrothermal biotite is correlative with the Fe/Fe+Mg+Mn ratio, but that this relationship

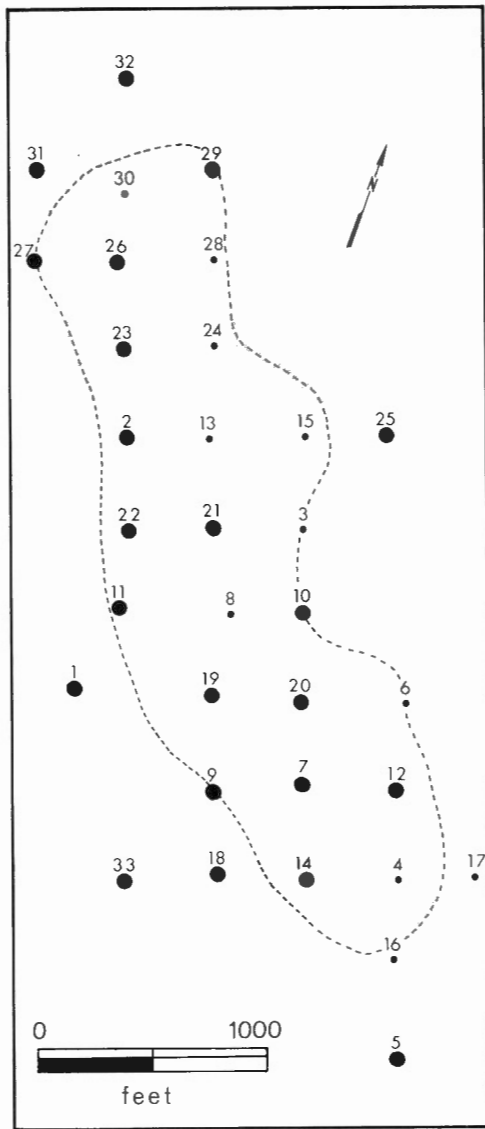


Figure 15. Relative abundances of pyrite in the upper 500 feet of the Maggie deposit drillholes. Large and small dots represent holes containing pyrite estimated to be >3% and <3% by volume, respectively.

is not maintained for greenish micas. The cause is most clearly shown by analyses 5a, 5b, 6a, and 6b for D. D. H. MM-24 at 817 feet (Appendix I). The colours of the micas are, in the above sequence, pale green, light brownish green, and medium brown. All have similar Fe/Fe+Mg+Mn ratios, but the pale green micas have anomalously high Al and low Ti in octahedral positions. As the brownish colour intensifies (6a and 6b), Al progressively decreases and Ti increases, with the latter being the obvious chromophore.

Biotite quality in relation to copper grades

Carson and Jambor (1974) have proposed that, in porphyry copper deposits in which biotitization is the

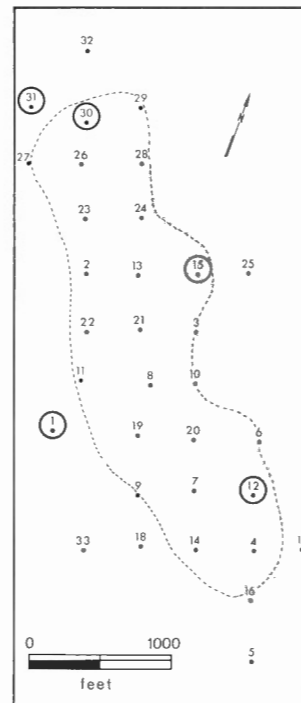


Figure 16
Drillholes in which tennantite was observed.

dominant type of potassic alteration (as at Maggie), the quality of biotitization is a reliable indicator of the grade of the Cu-Mo zone. At the Maggie deposit, the limited extent of dark brown, good quality hydrothermal biotite, and the prevalence of lighter coloured varieties, attest to the overall low grade of copper-molybdenum. Unfortunately, assay data for the drillholes are unavailable and thus detailed comparisons with the voluminous biotite analytical data are not possible. However, because the correlation between copper grades and the quality of biotitization has been found to be consistent in this type of deposit throughout the world (Carson and Jambor, 1974; unpublished data), the microscopically determined alteration has been used to predict the extent and detailed shape of the Maggie copper zone. The results, using an interpreted 0.2% Cu cut-off (as in Fig. 3), are given in four longitudinal sections (Figs. 20-23). These show that the copper zone is about 1300 by 300 metres in surface dimensions, has a shallow umbrella shape, and is wide and deep in the west. Successive eastward sections indicate that the zone thins appreciably, plunges west, and that a large portion of the southeastern part of the deposit is relatively thin. In general, the thickest intersections of copper zone lie towards the hanging wall of the quartz monzonite porphyry. Maximum grades in the interior of the deposit would appear to be about 0.5% Cu, but most of the deposit has biotitization typical of 0.2-0.4% Cu.

K-feldspar alteration

Most K-feldspar at the Maggie deposit is related to magmatic processes rather than to hydrothermal alteration. Microprobe analyses of narrow, corroded

Table 4
Clay mineral ratios in samples from Maggie deposit

D. D. H. No. and Footage	Clay Mineral Ratios			
	illite	kaolinite	montmorillonite	chlorite
MM- 4-591	20	15	65	-
-822	45	8	47	-
MM-13-710	7	79	14	-
-812	51	27	22	-
MM-14-387	82	5	-	13
-862	44	10	46	-
MM-17-556	55	17	28	-
-774	20	22	58	-
MM-18-872	45	3	41	11
-1497	28	18	54	-
MM-33-327	79	4	8	9
-582	41	33	26	-

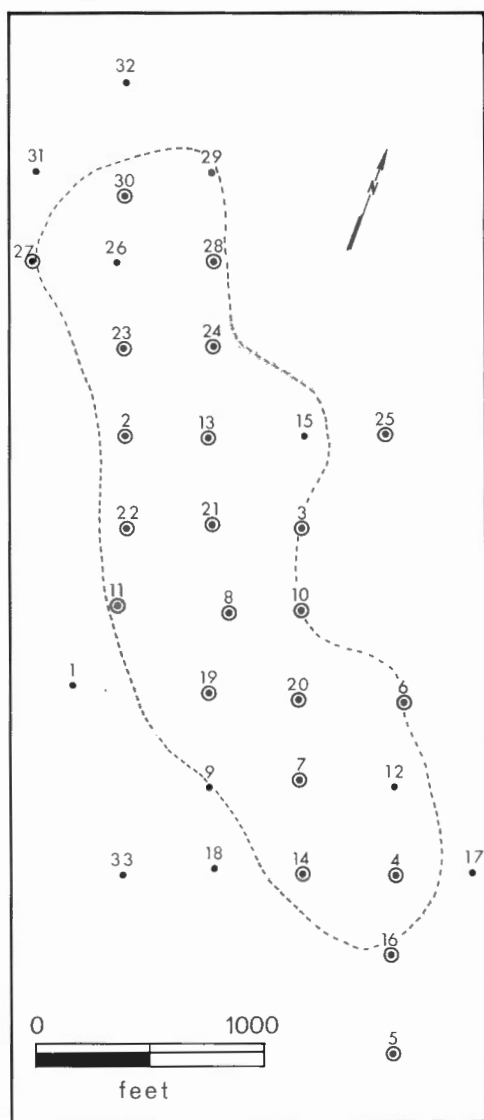


Figure 17 (left)

Distribution of hydrothermal biotite at bedrock surface (occurrences are shown as circles). With the exception of one outcrop near D. D. H. MM-1, hydrothermal biotite is present only in the drillhole area. All non-biotitized holes are characterized by the presence of strong sericitic alteration. See also Figures 20-23 for biotitization in vertical sections through the deposit.

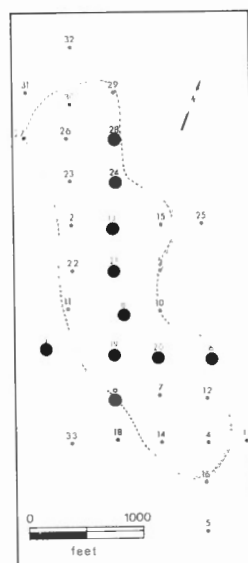


Figure 18

Location of the 10 drillholes (large dots) for which microprobe analyses of biotites are given in Appendix I.

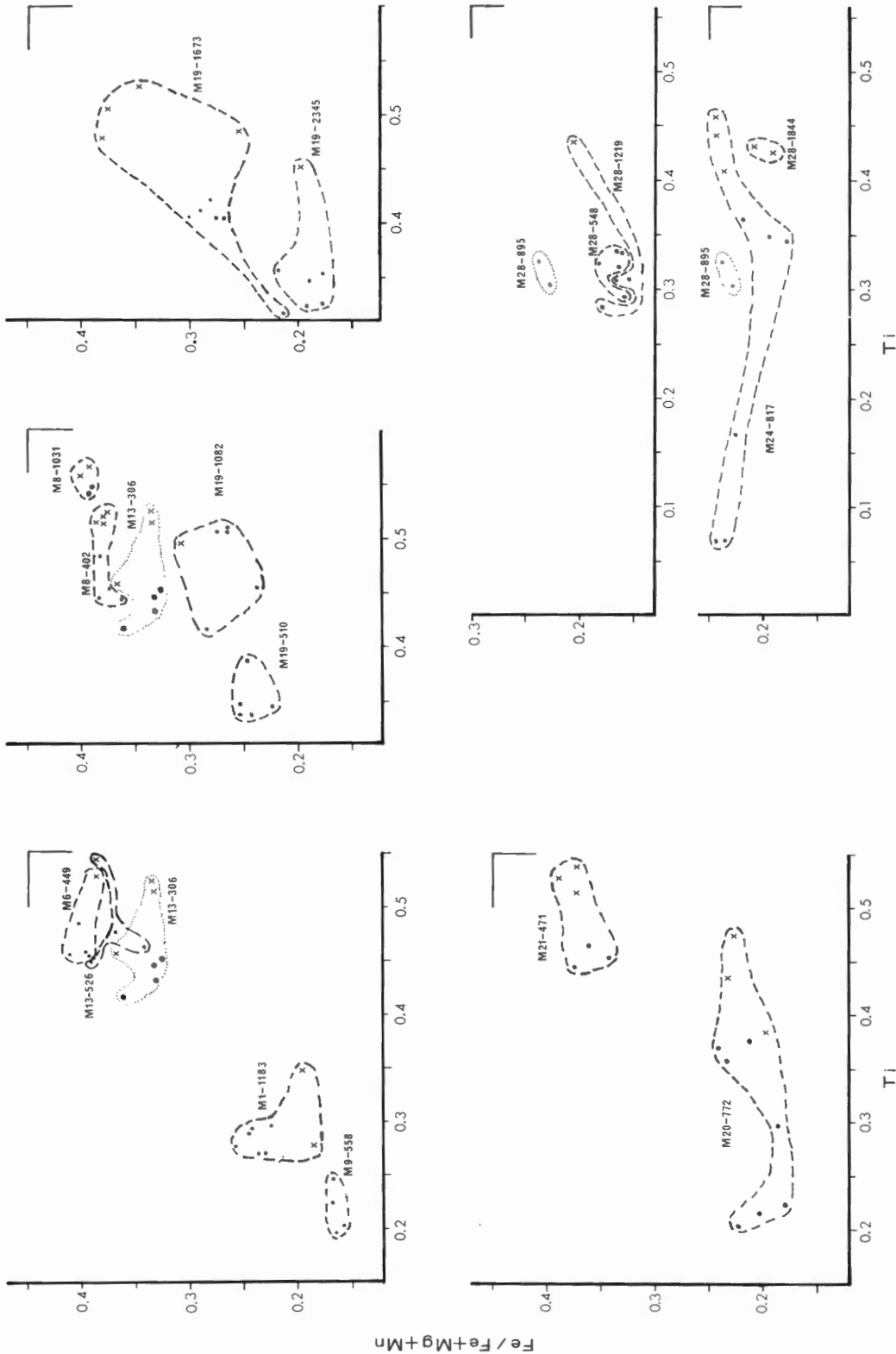


Figure 19. Ti versus Fe/(Fe+Mg+Mn) for hydrothermal biotites (dots) and phenocrysts (x's) from the Maggie deposit; values are based on microprobe analyses calculated to 22 oxygens as given in Appendix I. Analyses from each polished thin section are enclosed within dashes or dots, with the latter indicating that the sample is also plotted on an adjacent diagram in the figure. Note that phenocrysts are generally enriched in Ti relative to the associated hydrothermal biotites; however, the tendency for the analyses to cluster at different levels of Fe/(Fe+Mg+Mn) suggests that the phenocrysts also may have been affected by hydrothermal alteration.

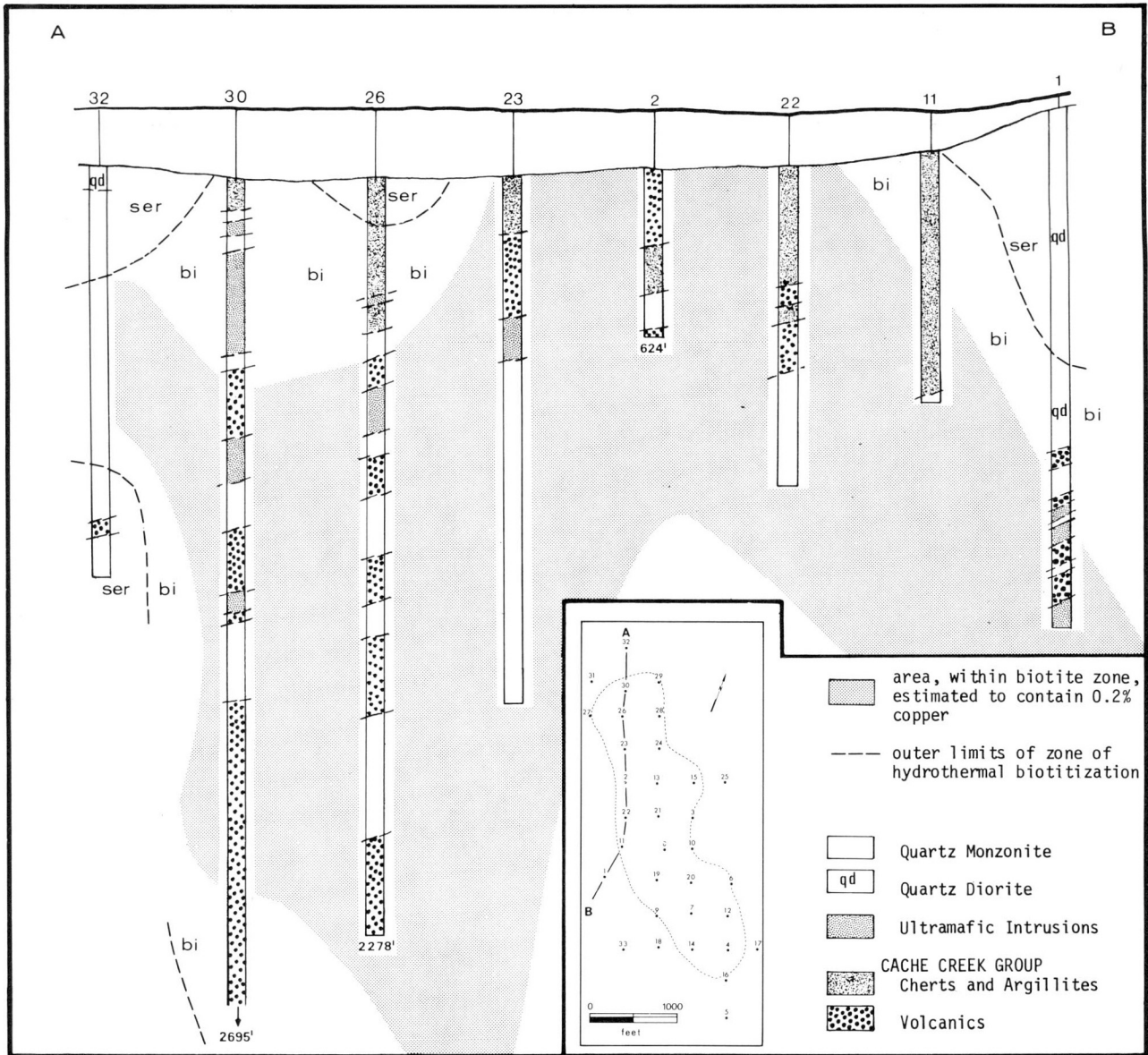


Figure 20. Limits of hydrothermal biotitization in longitudinal section A-B (inset). The shaded area contains better-quality hydrothermal biotite estimated to be correlative with the zone of +0.2% copper.

rims and microscopic veinlets that cut through plagioclase phenocrysts indicate that the material is generally albite in compositional continuity with the phenocrysts. In some cases, large perthitic grains are grouped along microscopic fractures; such grains may be of late-magmatic origin. A possibly related phenomenon, noted previously, is the tendency for rocks of granitic composition to have a medial distribution in the thicker parts of the quartz monzonite porphyry. These rocks may have been subjected to deuteric or hydrothermal effects, but it has not been possible to allocate the rocks to a specific position in the hydrothermal alteration scheme. However, some clearly hydrothermal, copper-bearing quartz veinlets do have sporadic K-feldspar grains at

their margins, and others enclose isolated grains and microscopic aggregates of K-feldspar and albite. Overall, potassic alteration of this type is neither conspicuous nor extensive at the Maggie deposit.

Silicification and sericitization

Quartz has two distinct modes of occurrence: (1) as quartz veinlets, 1 to 5 mm wide, that occur both inside and outside the copper zone; those inside generally carry chalcopyrite or molybdenite, whereas those outside are generally pyrite-bearing; (2) quartz, with associated sericite, that has flooded the host rocks and obliterated most of the original minerals and textures

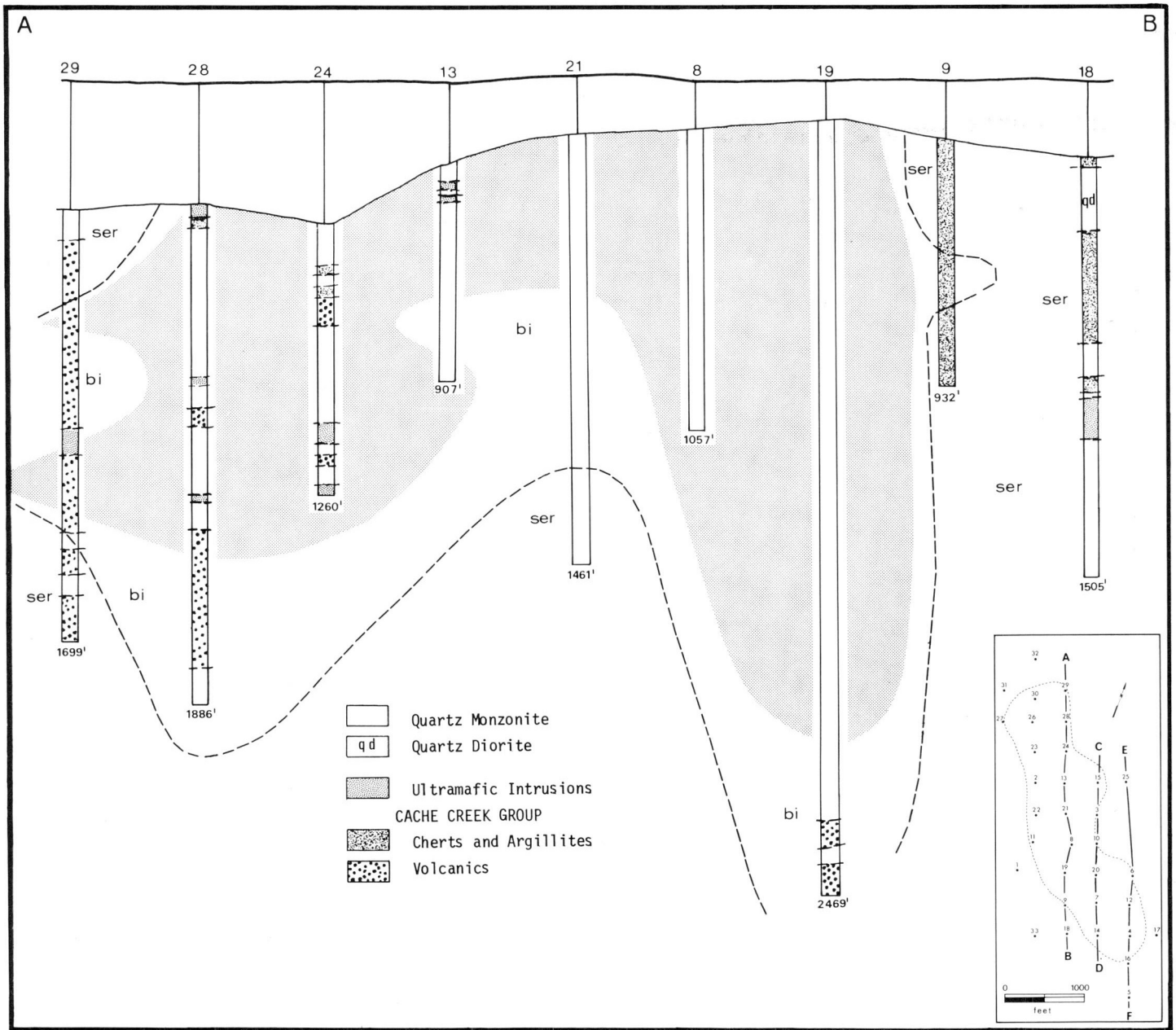


Figure 21. Section A-B (inset), showing the area (shaded) estimated to contain +0.2% copper. Legend is as in Figure 20.

except for the preservation of vague outlines of feldspar phenocrysts. This type of pervasive quartz flooding is characteristic of an intense quartz-sericite (phyllic) facies of hydrothermal alteration, whereas quartz veining is not restricted to a specific facies.

Quartz veining is categorized as being abundant where at least one average-sized veinlet is present per 7- to 10-cm length of drill core of intrusive porphyry; volcanic rocks have less veining than the porphyries, and the ultramafics have the least. Despite the imprecision expected because veinlet abundances were estimated largely from specimens available for laboratory

study, a readily-perceived pattern has emerged. As shown in Figure 24, quartz veining is clearly more abundant in the southeastern part of the copper zone than it is in the northwestern part. The southern concentration may be related to the prevalence of multiphase intrusion and brecciation in this area.

Shown also in Figure 24 are the drillhole occurrences of pervasive silicification. These are concentrated along the hanging wall of the deposit; outcrops to the southwest of the drillholes are also strongly silicified.

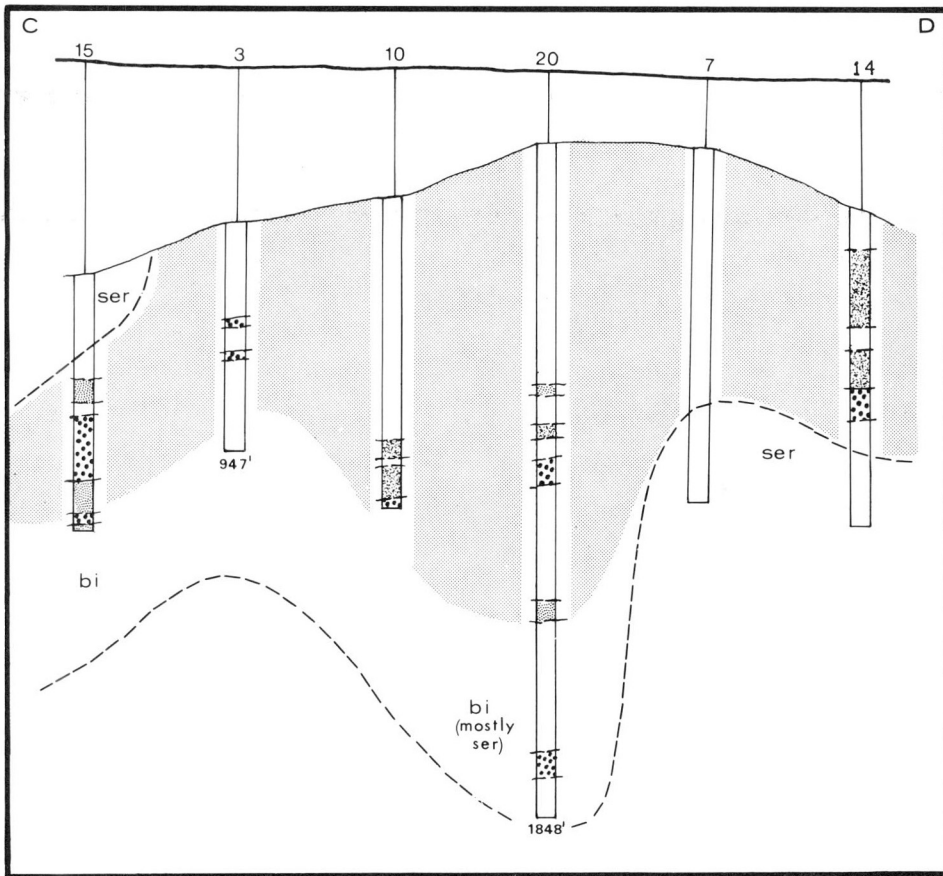


Figure 22
 Section C-D (inset of Fig. 21),
 with shaded area estimated to
 contain +0.2% copper. Legend
 is as in Figure 20.

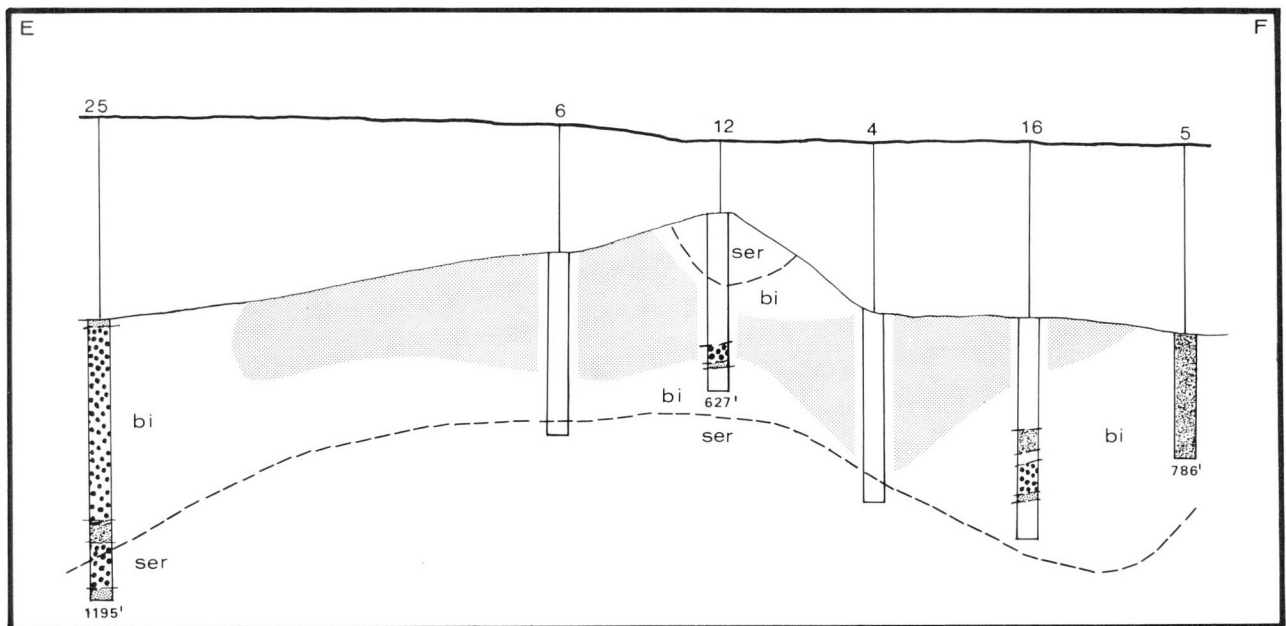


Figure 23. Section E-F (inset of Fig. 21), with shaded area estimated to contain +0.2% copper. Legend is as in Figure 20.

Figure 24

Distributions and relative abundances of quartz veining and silicification in the Maggie deposit drillholes: (a) in the upper parts of the holes, to depths of 500-600 feet below surface; (b) in the lower parts of the holes.

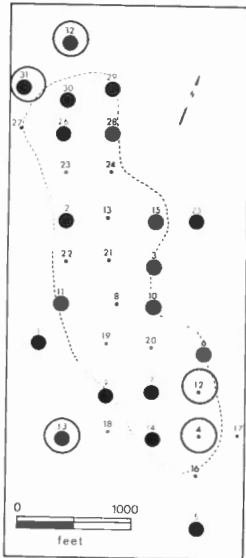
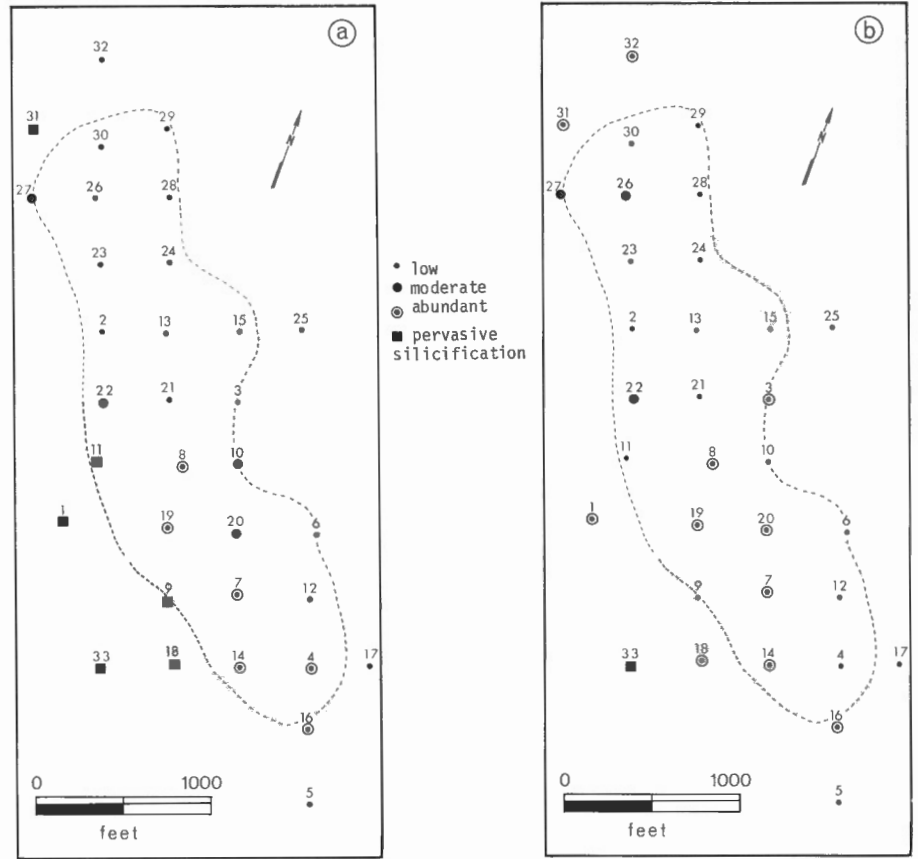


Figure 25

Distribution of carbonates in the Maggie deposit drillholes. Calcite occurrences are shown as large dots, and dolomite occurrences are shown as open circles. Note the absence of both of the carbonates in the central part of the copper zone, and the peripheral distribution of dolomite.

Argillic alteration

Drill cores of the rocks from the Maggie deposit appear megascopically to be much more extensively altered than rocks from the Babine Lake area. This impression is conveyed because clay alteration is developed more strongly at the Maggie deposit and because, unlike the predominance of kaolinite in the

Babine deposits, montmorillonite is abundant. Thus drill cores, especially of the quartz monzonite porphyry, are commonly pitted because of montmorillonite expansion and spalling, and some cores are totally disintegrated for lengths of more than 50 feet.

Representative clay-mineral analyses, using the procedure outlined in Jambor and Delabio (1975), are given in Table 4. The results confirm that montmorillonite is an abundant constituent of the clay fraction, and that the mineral occurs in the quartz diorite porphyry (D.D.H. MM-32) as well as in the quartz monzonite unit.

Megascopic examination of the drill core indicates that montmorillonite is developed only very poorly in Cache Creek rocks, is locally abundant in quartz diorite, and is common in quartz monzonite porphyries. The distribution of the mineral is in fact remarkably similar to the patterns shown for strong quartz veining (Fig. 24), that is, drillholes containing abundant quartz veins also have abundant montmorillonite, and those with little quartz have little montmorillonite. Cross-sections of the deposit also indicate that, although montmorillonite is locally abundant in the footwall of the quartz monzonite porphyry, the mineral occurs more consistently in the central, more salic part of the intrusion, and, to a lesser extent, along the hanging wall except where the finer grained phase of the intrusion is present.

Carbonate alteration

In the Maggie drillhole area, carbonate veinlets are present locally, but pervasive carbonate alteration is so conspicuously uncommon that special note was taken wherever more than a minute grain or two were observed in thin sections. Forty-five thin sections of drill cores were selected on this basis and were stained subsequently with alizarin red. Grains that gave a reaction other than for calcite were identified by X-ray powder diffraction patterns. Only calcite and dolomite were found.

The distribution of calcite and dolomite in the Maggie drillholes is shown in Figure 25, which indicates clearly that carbonate occurrences are rare or absent in the central part of the copper zone. Of the five drillholes that contain dolomite, three are outside the copper zone, and the other two (D. D. H. 4 and 12) are in a fine grained, dyke-like, breccia body that is low in copper.

As both calcite and dolomite are more common in outcrops that surround the copper zone, a zonal arrangement of the carbonates is present. The outward sequence from the central biotite- and copper-rich part of the deposit is: "barren" → calcite → calcite + dolomite. Although calcite overlaps the biotite zone, dolomite seems to appear only in sericitic (phyllic) and propylitic assemblages.

SUPERGENE ALTERATION

Very minor chalcocite was noted in near-surface drill core, but polished section studies do not indicate that any significant supergene enrichment has occurred. Iron oxides are conspicuous in the gossan of the weathered pyrite halo, and much of the yellowish coloration is due to the presence of abundant natrojarosite. Although minor gypsum occurs along fractures in the copper zone, the mineral is abundant in the weathered pyrite halo, where fractures commonly glisten because of gypsum coatings. In some of the regolith on the hanging wall of the deposit, gypsum is so plentiful that the soils appear to be frost-coated.

Only a few grains of non-sulphide copper minerals have been found. Brochantite is present and, despite the overwhelming sulphatic environment, malachite also has been noted.

CONCLUSIONS

The Maggie porphyry Cu-Mo deposit is similar to the "Babine-type" deposits in that the sulphides are related to Tertiary porphyritic intrusions, and in that the copper zone and hydrothermal biotitization are related intimately. Good quality, medium- to dark-brown hydrothermal biotites occur only within the estimated +0.2% Cu zone. Microprobe analyses indicate that the darker biotites generally have higher Fe/Fe+Mg+Mn ratios, and greenish biotites are low in titanium. Biotite phenocrysts generally contain more titanium than

the associated hydrothermal biotites, but similarities in Fe/Fe+Mg+Mn ratios suggest that some of the phenocrysts have been partly affected by hydrothermal alteration.

Although the Maggie deposit has normal sulphide zoning, consisting of an outward sequence of (bornite + chalcopyrite + pyrite) → (chalcopyrite + pyrite) → pyrite, an unusual feature is the occurrence of tennantite, which is concentrated at the periphery of the copper zone. The relatively poor development of sulphide zoning is indicated by the presence of abundant pyrite throughout the copper zone.

The non-sulphide hydrothermal alteration assemblages consist of an outward sequence of biotite → sericite ± quartz → chlorite ± carbonate. The biotite-sericite boundary generally marks the limit of the estimated +0.2% Cu zone. Clay alteration is common throughout the inner parts of the deposit, but does not have a specific relationship to sulphide zoning.

All porphyritic intrusions at the Maggie property are related closely, but sulphide minerals and hydrothermal alteration are associated with porphyritic quartz monzonite. Detailed studies of the quartz monzonite porphyry have indicated that it is multiphase, is variable in composition, and is partly inter-mineral. The youngest phase is in part a dyke-like body that contains abundant fluidized breccia. The dyke-like unit is predominantly sericitized and pyritized, and is locally intrusive into biotitized porphyry. The intrusion-alteration-mineralization relationships indicate that biotitization and copper deposition occurred largely before the complete cessation of intrusion, and that most of the porphyry system was at a "lower-grade" stage of metasomatic alteration when late dyke intrusion occurred.

REFERENCES

- Carson, D. J. T. and Jambor, J. L.
1974: Mineralogy, zonal relationships and economic significance of hydrothermal alteration at porphyry copper deposits, Babine Lake area, British Columbia; *Can. Min. Met. Bull.*, v. 67, p. 110-133.
- Deer, W. A., Howie, R. A., and Zussman, J.
1962: *Rock-forming minerals*; v. 3, Longmans, London.
- Duffell, S. and McTaggart, K. C.
1952: Ashcroft map-area, British Columbia; *Geol. Surv. Can.*, Mem. 262.
- Jacobs, D. C. and Parry, W. T.
1974: Geochemistry of biotite from the Santa Rita stock and its associated potassic and phyllic alteration zones, Central Mining District, Grant County, New Mexico; *Geol. Soc. Am. Ann. Mtg. Abstr.*, p. 809.

Jambor, J.L. and Delabio, R. N.

1975: Clay mineral variations in the Bell Copper porphyry copper deposit, Babine Lake area, B.C.; in Report of Activities, Pt. B, Geol. Surv. Can., Paper 75-1B.

Kirkham, R. V.

1971: Intermineral intrusions and their bearing on the origin of porphyry copper and molybdenum deposits; Econ. Geol., v. 66, p. 1244-1249.

McMillan, W. J.

1970: Maggie mine; B. C. Dept. Mines Pet. Resour., G.E.M. 1970, p. 324-325.

Miller, D.

1972: Unpublished geological map of the Maggie property; Bethlehem Copper Corporation, Limited, Vancouver, B.C.

Moore, W. J. and Czamanske, G. K.

1973: Compositions of biotites from unaltered and altered monzonitic rocks in the Bingham Mining District, Utah; Econ. Geol., v. 68, p. 269-274.

APPENDIX I

MICROPROBE ANALYSES OF BIOTITES FROM MAGGIE DEPOSIT

Descriptive Notes:

D. D. H. MM-1 at 1183 feet

- 1a, 1b : both grains are about 0.06 by 0.03 mm in size, pale brown, 0.3 mm apart, in a very large pseudomorph after amphibole
- 2 : 0.1 by 0.06 mm, pale brown, probably part of a large pseudomorph
- 3a, b, c: three laths approximately 0.05 by 0.10 mm in an area 0.3 by 0.4 mm; light brown, coarse sucrose pseudomorph
- 4, 5 : two phenocrysts, 1 by 1.5 mm and 7 mm apart; partly rutilated, but analyzed on fresh areas

D. D. H. MM-8 at 402 feet

- 1a : phenocryst, 0.4 by 1.0 mm
- 1b : single, isolated lath, 0.04 by 0.12 mm, 7 mm from 1a; grain looks like a non-sucrose, single-grain pseudomorph after amphibole
- 1c : 0.4 mm from 1b, very dark brown lath 0.05 by 0.14 mm that is part of a large amphibole pseudomorph
- 2, 3, 4 : three large, normal phenocrysts
- 5, 6 : two very dark brown laths, 0.04 by 0.14 and 0.05 by 0.08 mm respectively, from two pseudomorphs at opposite sides of the thin section

D. D. H. MM-8 at 1031 feet

- 1 : dark brown grain 0.06 by 0.06 mm, isolated in matrix
- 2 : normal phenocryst
- 3 : long lath, 0.07 by 0.14 mm, probably a pseudomorph
- 4 : normal phenocryst

D. D. H. MM-6 at 449 feet

- 1a, b : grain (a) 0.07 by 0.04 mm, part of very dark brown sucrose pseudomorph; grain (b) 0.5 mm away, isolated in matrix
- 2a, b : two laths, 0.04 by 0.07 mm and 0.2 mm apart, in a sucrose pseudomorph
- 3 : phenocryst, 1.0 by 1.5 mm

D. D. H. MM-9 at 558 feet

- 1a, b : lath 0.03 by 0.12 mm, in massively biotitized matrix of volcanic; grain 1b 0.7 mm from 1a
- 2a, b : light brown lath 0.03 by 0.13 mm; grain 2b is a basal section of larger grain, almost in contact with 2a

D. D. H. MM-13 at 306 feet

- 1a, b : two phenocrysts, 2 by 1 mm and 1.0 by 0.5 mm respectively, in mutual contact
- 2a, b : two laths 0.06 by 0.18 mm and 0.3 mm apart; dark brown; part of sucrose pseudomorph
- 3 : lath 0.05 by 0.12 mm, probably part of a pseudomorph
- 4a : coarse lath 0.1 by 0.2 mm, part of sucrose pseudomorph
- 4b : phenocryst (?) 1.0 by 0.8 mm, probably part of basal section of a larger grain

D. D. H. MM-13 at 526 feet

- 1 : dark brown lath, 0.13 by 0.65 mm; appears to be part of a pseudomorph; other grains of hydrothermal biotite in this thin section are also unusually coarse
- 2 : basal section of large lath similar to above; uncertain texturally whether phenocryst or hydrothermal
- 3 : irregular phenocryst, 1.0 by 0.7 mm, with corroded edges
- 4 : lath 0.05 by 0.1 mm, part of sucrose pseudomorph

Descriptive Notes (cont'd.)

D. D. H. MM-13 at 873 feet

- 1a : lath 0.03 by 0.1 mm, probably part of a pseudomorph
- 1b : grain 0.1 by 0.1 mm in contact with above
- 2a, b : two phenocrysts in contact, 1.0 by 0.7 mm
- 3 : coarse, irregular grain 0.11 by 0.13 mm, probable pseudomorph

Grain 1b has Ti similar to phenocrysts, but Fe/Fe+Mg+Mn ratio is closer to those of hydrothermal biotites

D. D. H. MM-19 at 510 feet

- 1 : lath 0.04 by 0.08 mm, moderately dark brown; probably part of pseudomorph
- 2 : similar to 1 above, 1.5 cm away
- 3 : isolated grain 0.04 by 0.1 mm, in matrix
- 4 : lath, 0.04 by 0.2 mm, part of pseudomorph and about 10 times larger than associated grains
- 5 : lath 0.03 by 0.06 mm, in matrix

D. D. H. MM-19 at 1082 feet

- 1a : basal section, part of sucrose pseudomorph
- 1b : moderately dark brown lath, 0.02 by 0.04 mm; 0.15 mm from 1a
- 2 : phenocryst, 0.5 by 0.5 mm
- 3a, b : lath, 0.06 by 0.17 mm, part of coarse sucrose pseudomorph; grain 3b similar, 0.3 mm away
- 4 : lath in matrix, 0.04 by 0.07 mm

D. D. H. MM-19 at 1673 feet

- 1a, b : adjacent moderately dark brown laths, 0.25 mm apart, in sucrose pseudomorph; each lath about 0.05 by 0.10 mm
- 2 : fresh area in 0.25 by 0.35 mm phenocryst, chloritized along cleavages, with residual rutile needles
- 3 : lath, 0.03 by 0.05 mm, in sucrose pseudomorph; not as dark brown as area 1
- 4a, b, c : dark brown lath, 0.08 by 0.15 mm, probably part of pseudomorph; grain 4b similar, 0.3 mm from above; grain 4c is 0.04 by 0.14 mm lath in contact with 4b
- 5, 6, 7 : phenocrysts

D. D. H. MM-19 at 2345 feet

- 1 : phenocryst, 1 by 1.3 mm
- 2 : lath in matrix
- 3a, b : both medium brown, 0.07 by 0.02 mm, part of sucrose pseudomorph
- 4 : 0.06 by 0.08 mm lath, part of pseudomorph
- 5 : 0.06 by 0.2 mm lath in matrix

D. D. H. MM-20 at 772 feet

- 1a : phenocryst, 0.7 by 1.3 mm, partly rutilated
- 1b : medium brown lath, 0.06 by 0.2 mm, probably hydrothermal, in contact with phenocryst 1a
- 2 : medium brown lath, 0.05 by 0.1 mm; part of pseudomorph
- 3 : lath, 0.05 by 0.17 mm, part of coarse sucrose pseudomorph; slightly darker brown than 2
- 4 : phenocryst, 1.7 by 2.0 mm
- 5 : light brown lath, 0.06 by 0.15 mm; part of compact biotite mass forming 1/3 of thin section (biotitized inclusion?)
- 6a, b : in biotitized mass with 5, but grain 6a is a darker lath 0.09 by 0.23 mm; grain b is a basal section in contact with 6a
- 7a, b : phenocryst, 1 by 1.2 mm, in biotitized mass; 7b is in contact with 7a, but is a lath 0.04 by 0.15 mm; colour similar to that of grain 5

Descriptive Notes (cont'd.)

D. D. H. MM-21 at 471 feet

- 1 : lath 0.08 by 0.17 mm, part of pseudomorph
- 2 : small dark brown lath, 0.02 by 0.10 mm, in matrix
- 3, 4 : phenocrysts
- 5a, b : phenocryst (a), and grain 0.06 by 0.09 mm in contact, possibly pseudomorph

D. D. H. MM-24 at 817 feet

- 1 : coarse lath 0.07 by 0.4 mm, adjacent to a phenocryst; probably hydrothermal
- 2, 3 : phenocrysts at opposite sides of the thin section
- 4a, b : lath (a) 0.05 by 0.17 mm, probably pseudomorph; grain 4b seems to be a small phenocryst, 0.3 by 0.4 mm, surrounded by hydrothermal biotite
- 5a, b : pale green grain, 0.05 by 0.05 mm, in matrix; grain 5b is similar, but a basal section 0.06 by 0.12 mm, and 0.3 mm from 5a
- 6a : lath 0.05 by 0.05 mm, in matrix; light brownish green
- 6b : brown lath, 0.03 by 0.07 mm, in matrix; 0.6 mm from 6a

D. D. H. MM-28 at 548 feet

- 1 : lath 0.05 by 0.1 mm; probably part of pseudomorph
- 2 : similar, 1 mm from above and probably part of same pseudomorph
- 3a, b : anomalously large grain; 0.1 by 0.2 mm, probably part of pseudomorph; grain 3b is 0.1 mm from 3a and is 1/3 the size of 3a
- 4 : lath 0.07 by 0.15 mm, part of pseudomorph

D. D. H. MM-28 at 895 feet

- 1, 2 : pale to medium brown laths in two pseudomorphs

D. D. H. MM-28 at 1219 feet

- 1 : pale brown lath, probably part of a pseudomorph
- 2 : phenocryst, 1 by 1 mm
- 3a, b : two coarse laths, 0.07 by 0.12 mm, part of a large pseudomorph

D. D. H. MM-28 at 1844 feet

- 1, 2 : large phenocryst, 2.4 by 3.6 mm; areas 1 and 2 at opposite sides of the grain

Microprobe Analyses of Biotites from Maggie deposit*

D.D.H. MM-1 at 1183 feet										D.D.H. MM-8 at 402 feet									
Wt. %	1a	1b	2	3a	3b	3c	4	5	1a	1b	1a	1b	1a	1b	1a	1b			
SiO ₂	38.83	38.68	38.11	38.34	37.95	36.56	38.42	37.84	37.31	37.95	37.31	37.95	37.31	37.95	37.31	37.95			
TiO ₂	2.45	2.66	2.66	2.45	2.58	2.39	2.50	3.14	4.54	4.27	4.54	4.27	4.54	4.27	4.54	4.27			
Al ₂ O ₃	14.72	14.14	15.31	15.39	15.22	14.77	14.91	15.29	13.30	13.15	13.30	13.15	13.30	13.15	13.30	13.15			
Cr ₂ O ₃	0.04	0.04	0.05	0.05	0.05	0.08	0.00	0.05	0.02	0.00	0.02	0.00	0.02	0.00	0.02	0.00			
FeO	9.89	9.51	10.28	10.07	10.31	10.41	7.87	8.15	16.40	15.85	16.40	15.85	16.40	15.85	16.40	15.85			
MnO	0.12	0.04	0.22	0.16	0.04	0.10	0.03	0.00	0.18	0.07	0.18	0.07	0.18	0.07	0.18	0.07			
MgO	18.44	18.39	17.72	18.07	17.71	16.93	19.39	18.68	14.67	14.34	14.67	14.34	14.67	14.34	14.67	14.34			
CaO	0.13	0.20	0.12	0.11	0.09	0.13	0.11	0.08	0.01	0.04	0.01	0.04	0.01	0.04	0.01	0.04			
Na ₂ O	0.31	0.38	0.75	0.64	0.53	0.52	0.62	0.48	0.37	0.34	0.37	0.34	0.37	0.34	0.37	0.34			
K ₂ O	9.95	9.73	10.09	10.14	9.90	9.75	9.72	9.73	9.20	9.65	9.20	9.65	9.20	9.65	9.20	9.65			
Total	94.88	93.77	95.31	95.42	94.38	91.64	93.57	93.44	96.00	95.66	96.00	95.66	96.00	95.66	96.00	95.66			
Numbers of ions on the basis of 22 oxygens																			
Si	5.693	5.727	5.595	5.611	5.613	5.593	5.658	5.590	5.585	5.688	5.585	5.688	5.585	5.688	5.585	5.688			
Al	2.307	2.273	2.405	2.389	2.387	2.407	2.342	2.410	2.347	2.312	2.347	2.312	2.347	2.312	2.347	2.312			
Al	0.236	0.194	0.245	0.265	0.267	0.256	0.246	0.253	0.000	0.011	0.000	0.011	0.000	0.011	0.000	0.011			
Ti	0.270	0.296	0.294	0.270	0.287	0.275	0.277	0.349	0.511	0.481	0.511	0.481	0.511	0.481	0.511	0.481			
Cr	0.005	0.005	0.006	0.006	0.006	0.010	-----	0.006	0.002	-----	0.002	-----	0.002	-----	0.002	-----			
Fe ²⁺	1.213	1.178	1.262	1.232	1.275	1.332	0.969	1.007	2.053	1.987	2.053	1.987	2.053	1.987	2.053	1.987			
Mn	0.015	0.005	0.027	0.020	0.005	0.013	0.004	-----	0.023	0.009	0.023	0.009	0.023	0.009	0.023	0.009			
Mg	4.030	4.059	3.878	3.942	3.905	3.861	4.257	4.114	3.274	3.204	3.274	3.204	3.274	3.204	3.274	3.204			
Ca	0.020	0.032	0.019	0.017	0.014	0.021	0.017	0.013	0.002	0.006	0.002	0.006	0.002	0.006	0.002	0.006			
Na	0.088	0.109	0.214	0.182	0.152	0.154	0.177	0.138	0.107	0.099	0.107	0.099	0.107	0.099	0.107	0.099			
K	1.861	1.838	1.890	1.893	1.868	1.903	1.826	1.834	1.757	1.845	1.757	1.845	1.757	1.845	1.757	1.845			
Fe																			
Fe+Mg+Mn	0.231	0.225	0.244	0.237	0.246	0.256	0.185	0.197	0.384	0.382	0.384	0.382	0.384	0.382	0.384	0.382			

*Analyst A.G. Plant. Total Fe as FeO.

D.D.H. MM-8 at 402 feet (cont'd.)

D.D.H. MM-8 at 1031 feet

Wt. %	1c	2	3	4	5	6	1	2	3	4
SiO ₂	37.86	37.10	36.89	37.09	38.64	38.04	37.50	37.25	37.50	37.16
TiO ₂	3.99	4.59	4.51	4.61	3.94	3.97	4.83	4.93	4.78	5.04
Al ₂ O ₃	12.92	13.02	13.30	13.18	12.49	13.43	13.17	13.36	13.91	13.16
Cr ₂ O ₃	0.00	0.00	0.01	0.01	0.03	0.02	0.00	0.00	0.02	0.01
FeO	15.81	16.18	16.20	15.92	15.47	16.10	15.79	16.66	15.82	16.71
MnO	0.14	0.09	0.13	0.12	0.14	0.12	0.07	0.09	0.13	0.07
MgO	14.74	14.77	14.65	14.60	15.24	14.43	13.81	13.91	13.65	14.58
CaO	0.05	0.01	0.04	0.02	0.04	0.04	0.05	0.02	0.04	0.05
Na ₂ O	0.39	0.62	0.61	0.64	0.35	0.48	0.64	0.48	0.38	0.45
K ₂ O	9.36	9.26	9.23	9.28	9.47	9.49	8.98	9.22	8.77	9.28
Total	95.26	95.64	95.57	95.47	95.81	96.12	94.84	95.92	95.00	96.51

Numbers of ions on the basis of 22 oxygens

Si	5.694	7.984	7.888	7.915	7.921	7.958	5.658	5.588	7.951	5.548
Al	2.290	2.308	2.360	2.338	2.195	2.325	2.342	2.362	2.369	2.316
Al	0.000	0.000	0.000	0.000	0.000	0.037	0.001	0.000	0.093	0.000
Ti	0.451	0.519	0.511	0.522	0.442	0.445	0.548	0.556	0.540	0.566
Cr	-----	5.762	5.878	5.857	5.818	5.781	-----	-----	5.769	0.001
Fe ²⁺	1.989	2.035	2.040	2.004	1.929	2.009	1.993	2.090	1.987	2.086
Mn	0.018	0.011	0.017	0.015	0.018	0.015	0.009	0.011	0.017	0.009
Mg	3.305	3.312	3.288	3.276	3.388	3.209	3.106	3.111	3.056	3.245
Ca	0.008	0.002	0.006	0.003	0.006	0.006	0.008	0.003	0.006	0.008
Na	0.114	1.918	1.959	0.187	1.972	1.909	0.187	1.924	1.907	0.130
K	1.796	1.777	1.773	1.782	1.802	1.806	1.729	1.765	1.680	1.768
Fe										
Fe+Mg+Mn	0.374	0.380	0.382	0.378	0.362	0.384	0.390	0.401	0.393	0.391

D.D.H. MM-6 at 449 feet

D.D.H. MM-9 at 558 feet

Wt. %	1a	1b	2a	2b	3	1a	1b	2a	2b
SiO ₂	37.49	38.72	36.81	38.67	37.19	37.98	39.43	39.32	39.03
TiO ₂	3.99	4.10	4.18	4.10	4.71	1.85	1.80	2.21	2.00
Al ₂ O ₃	13.56	13.03	12.77	13.74	13.45	14.58	15.04	14.85	14.74
Cr ₂ O ₃	0.00	0.00	0.01	0.01	0.00	0.06	0.04	0.12	0.02
FeO	16.72	16.84	16.36	16.32	16.55	6.89	7.03	6.91	7.05
MnO	0.00	0.00	0.00	0.01	0.04	0.00	0.04	0.02	0.00
MgO	13.51	14.61	13.69	14.01	14.90	20.41	20.12	19.19	19.65
CaO	0.07	0.04	0.05	0.06	0.02	0.10	0.14	0.12	0.14
Na ₂ O	0.42	0.47	0.55	0.45	0.55	0.50	0.53	0.43	0.46
K ₂ O	9.29	9.26	9.24	9.48	9.25	9.74	9.99	9.86	9.69
Total	95.05	97.07	93.66	96.85	96.66	93.91	94.16	93.03	92.78

Numbers of ions on the basis of 22 oxygens

Si	5.669	5.720	5.660	5.713	5.536	5.789	5.739	5.782	5.758
Al	2.331	2.269	2.315	2.287	2.360	2.211	2.261	2.218	2.242
Al	0.086	0.000	0.000	0.106	0.000	0.289	0.319	0.356	0.321
Ti	0.454	0.456	0.483	0.456	0.527	0.202	0.197	0.244	0.222
Cr	-----	-----	0.001	0.001	-----	0.007	0.005	0.014	0.002
Fe ²⁺	2.115	2.081	2.104	2.017	2.060	0.839	0.856	0.850	0.870
Mn	-----	-----	-----	0.001	0.005	-----	0.005	0.002	-----
Mg	3.045	3.218	3.138	3.086	3.306	4.427	4.366	4.207	4.322
Ca	0.011	0.006	0.008	0.009	0.003	0.016	0.022	0.019	0.022
Na	0.123	0.135	0.164	0.129	0.159	0.141	0.150	0.123	0.132
K	1.792	1.745	1.813	1.787	1.757	1.808	1.855	1.850	1.824
Fe	-----	-----	-----	-----	-----	-----	-----	-----	-----
Fe+Mg+Mn	0.410	0.393	0.401	0.395	0.384	0.159	0.164	0.168	0.168

D.D.H. MM-13 at 306 feet

D.D.H. MM-13 at 526 feet

Wt. %	1a	1b	2a	2b	3	4a	4b	1	2	3
SiO ₂	36.86	37.80	38.25	38.05	37.75	38.00	37.06	38.31	36.26	36.95
TiO ₂	4.58	4.58	4.03	3.97	3.76	3.66	3.96	4.17	4.08	4.77
Al ₂ O ₃	13.19	13.49	13.03	13.24	12.44	13.27	13.03	13.19	12.29	13.12
Cr ₂ O ₃	0.00	0.00	0.00	0.01	0.00	0.01	0.00	0.04	0.00	0.04
FeO	13.74	14.06	13.95	14.06	13.75	14.59	14.82	14.93	15.27	15.99
MnO	0.05	0.01	0.09	0.05	0.07	0.13	0.04	0.05	0.05	0.06
MgO	15.13	15.81	15.98	15.78	15.45	14.41	14.20	16.09	14.55	14.22
CaO	0.12	0.02	0.09	0.00	0.03	0.09	0.11	0.15	0.13	0.07
Na ₂ O	0.60	0.55	0.41	0.53	0.48	0.53	0.71	0.57	0.51	0.53
K ₂ O	9.29	9.68	9.74	9.73	9.59	9.75	9.53	9.47	9.22	9.33
Total	93.56	96.00	95.57	95.42	93.32	94.44	93.46	96.97	92.36	95.08

Numbers of ions on the basis of 22 oxygens

Si	5.606	7.970	7.961	5.691	7.976	5.674	8.000	5.753	7.988	5.742	8.000	5.678	8.000	5.637	7.924	7.924	5.641	7.895	5.588	7.926
Al	2.365	2.357	2.285	2.285	2.285	2.326	2.326	2.235	2.258	2.258	2.322	2.322	2.322	2.287	2.254	2.254	2.254	2.254	2.339	2.339
Al	0.000	0.000	0.000	0.000	0.000	0.001	0.001	0.000	0.105	0.105	0.031	0.031	0.031	0.000	0.000	0.000	0.000	0.000	0.000	0.000
Ti	0.524	0.511	0.451	0.451	0.431	0.445	0.431	0.431	0.416	0.416	0.456	0.456	0.456	0.461	0.477	0.477	0.477	0.477	0.542	0.542
Cr	5.708	5.749	5.749	5.742	5.715	5.703	5.628	5.634	5.634	5.634	5.634	5.634	5.634	5.634	5.634	5.634	5.634	5.634	5.845	5.783
Fe ²⁺	1.748	1.743	1.736	1.753	1.753	1.753	1.753	1.753	1.844	1.844	1.899	1.899	1.899	1.837	1.987	1.987	1.987	1.987	2.022	2.022
Mn	0.006	0.001	0.011	0.006	0.009	0.017	0.017	0.009	0.017	0.017	0.005	0.005	0.005	0.006	0.007	0.007	0.007	0.007	0.008	0.008
Mg	3.430	3.494	3.544	3.508	3.510	3.544	3.508	3.510	3.246	3.246	3.243	3.243	3.243	3.529	3.375	3.375	3.375	3.375	3.206	3.206
Ca	0.020	0.003	0.014	0.014	0.005	0.015	0.015	0.015	0.015	0.015	0.018	0.018	0.018	0.024	0.022	0.022	0.022	0.022	0.011	0.011
Na	0.177	1.999	1.992	0.158	2.004	0.153	2.004	0.142	2.011	2.011	2.049	2.049	2.049	0.163	1.964	1.964	1.964	1.964	0.155	1.967
K	1.803	1.831	1.849	1.851	1.865	1.879	1.863	1.865	1.879	1.879	1.863	1.863	1.863	1.778	1.830	1.830	1.830	1.830	1.800	1.800
Fe																				
Fe+Mg+Mn	0.337	0.333	0.328	0.333	0.332	0.361	0.369	0.332	0.361	0.361	0.369	0.369	0.369	0.342	0.370	0.370	0.370	0.370	0.386	0.386

D.D.H. MM-13 at 526 feet (cont'd.)

D.D.H. MM-13 at 873 feet

D.D.H. MM-19 at 510 feet

Wt. %	4	1a	1b	2a	2b	3	1	2	3	4
SiO ₂	37.31	38.28	37.48	37.21	37.72	37.86	37.19	38.93	37.32	36.93
TiO ₂	3.93	4.34	4.63	4.64	4.56	4.07	3.01	3.09	3.45	3.04
Al ₂ O ₃	13.06	13.36	13.48	13.38	13.36	13.40	13.64	15.18	14.73	14.27
Cr ₂ O ₃	0.01	0.00	0.03	0.00	0.00	0.01	0.00	0.00	0.03	0.00
FeO	16.24	12.01	12.51	16.03	16.08	10.88	9.27	10.72	10.26	10.48
MnO	0.10	0.10	0.12	0.10	0.10	0.00	0.00	0.09	0.03	0.01
MgO	14.16	16.64	15.81	14.18	14.23	16.83	17.98	17.68	17.50	17.25
CaO	0.08	0.14	0.04	0.07	0.10	0.00	0.09	0.12	0.13	0.16
Na ₂ O	0.28	0.58	0.48	0.44	0.67	0.40	0.35	0.64	0.55	0.46
K ₂ O	9.60	9.61	9.70	9.18	9.39	9.57	9.64	10.07	9.92	9.63
Total	94.77	95.06	94.28	95.23	96.21	93.02	91.17	96.52	93.92	92.23

Numbers of ions on the basis of 22 oxygens

Si	5.665	8.000	5.672	8.000	5.624	8.000	5.605	7.981	5.629	7.980	5.696	8.000	5.675	8.000	8.000	5.563	8.000	5.638	8.000	5.632	8.000	5.607	8.000	
Al	2.335	2.328	2.376	2.376	2.376	2.376	2.376	2.350	2.350	2.304	2.304	2.325	2.325	2.325	2.362	2.437	2.437	2.362	2.362	2.437	2.437	2.393	2.393	
Al	0.003	0.005	0.008	0.000	0.000	0.000	0.000	0.000	0.000	0.072	0.072	0.129	0.129	0.229	0.229	0.150	0.150	0.229	0.229	0.150	0.150	0.160	0.160	
Ti	0.449	0.484	0.522	0.526	0.512	0.461	0.345	0.345	0.512	0.461	0.461	0.345	0.345	0.337	0.337	0.387	0.387	0.337	0.337	0.387	0.387	0.347	0.347	
Cr	0.001	-----	0.004	-----	-----	0.001	-----	-----	-----	0.001	0.001	-----	-----	-----	-----	0.004	0.004	-----	-----	0.004	0.004	-----	-----	
Fe ²⁺	2.062	5.733	1.488	5.664	1.570	5.565	2.020	5.742	2.007	5.697	1.369	5.678	1.183	1.298	1.298	5.691	1.279	5.748	1.298	5.691	1.279	5.712	1.331	
Mn	0.013	0.013	0.015	0.013	0.013	-----	0.013	0.013	0.013	-----	-----	-----	-----	0.011	0.011	0.004	0.004	0.011	0.011	0.004	0.004	0.001	0.001	
Mg	3.205	3.675	3.536	3.184	3.166	3.775	4.090	3.775	3.166	3.775	3.775	4.090	3.817	3.817	3.817	3.888	3.888	3.817	3.817	3.888	3.888	3.904	3.904	
Ca	0.013	0.022	0.006	0.011	0.016	-----	0.011	0.016	0.016	-----	-----	0.015	0.015	0.019	0.019	0.021	0.021	0.019	0.019	0.021	0.021	0.026	0.026	
Na	0.082	1.955	0.167	2.005	0.140	2.003	0.129	1.904	0.194	1.998	0.117	1.954	0.104	1.995	0.180	2.059	0.159	2.066	0.180	2.059	0.159	2.066	0.135	2.027
K	1.860	1.817	1.857	1.764	1.788	1.837	1.877	1.877	1.788	1.837	1.837	1.877	1.877	1.860	1.860	1.886	1.886	1.860	1.860	1.886	1.886	1.865	1.865	
Fe	-----	-----	-----	-----	-----	-----	-----	-----	-----	-----	-----	-----	-----	-----	-----	-----	-----	-----	-----	-----	-----	-----	-----	-----
Fe+Mg+Mn	0.391	0.288	0.306	0.387	0.387	0.266	0.224	0.224	0.387	0.266	0.266	0.224	0.224	0.253	0.253	0.247	0.247	0.253	0.253	0.247	0.247	0.254	0.254	

D.D.H. MM-19 at
510 feet (cont'd.)

D.D.H. MM-19 at 1082 feet

D.D.H. MM-19 at 1673 feet

Wt. %	5	1a	1b	2	3a	3b	4	1a	1b	2
SiO ₂	38.22	37.85	37.63	37.93	37.56	37.92	36.62	38.07	38.44	37.07
TiO ₂	3.01	4.03	4.48	4.34	4.52	4.55	3.63	3.75	3.66	4.64
Al ₂ O ₃	14.09	14.37	14.13	14.38	14.05	14.27	14.35	14.37	15.08	13.71
Cr ₂ O ₃	0.00	0.00	0.00	0.01	0.01	0.00	0.04	0.03	0.00	0.04
FeO	10.16	9.40	10.44	12.50	11.30	10.95	11.33	11.42	11.37	14.33
MnO	0.00	0.00	0.00	0.00	0.09	0.00	0.03	0.00	0.05	0.08
MgO	17.80	16.83	16.09	15.69	16.70	16.82	15.96	16.28	16.52	14.99
CaO	0.10	0.19	0.07	0.11	0.08	0.08	0.11	0.11	0.13	0.07
Na ₂ O	0.69	0.50	0.42	0.29	0.40	0.40	0.84	0.40	0.50	0.69
K ₂ O	9.76	9.52	10.07	9.59	9.62	9.59	9.63	9.60	9.92	9.16
Total	93.83	92.69	93.33	94.84	94.34	94.58	92.54	94.03	95.67	94.78

Numbers of ions on the basis of 22 oxygens

Si	5.685	8.000	5.669	8.000	5.631	8.000	5.609	8.000	5.672	8.000	5.571	7.999
Al	2.315	2.331	2.353	2.369	2.409	2.391	2.424	2.328	2.369	2.429	2.429	
Al	0.155	0.206	0.146	0.148	0.056	0.097	0.151	0.195	0.235	0.000	0.000	
Ti	0.337	0.454	0.506	0.485	0.506	0.506	0.416	0.420	0.403	0.524	0.524	
Cr	-----	5.702	-----	5.561	0.001	5.686	0.005	0.004	-----	0.005	0.005	5.699
Fe ²⁺	1.264	1.178	1.310	1.552	1.407	1.355	1.443	1.423	1.393	1.801	1.801	
Mn	-----	-----	-----	-----	0.011	-----	0.004	-----	0.006	0.010	0.010	
Mg	3.947	3.758	3.599	3.472	3.705	3.709	3.623	3.616	3.608	3.358	3.358	
Ca	0.016	0.030	0.011	0.017	0.013	0.013	0.018	0.018	0.020	0.011	0.011	
Na	0.199	2.067	1.995	0.083	1.917	0.115	1.937	0.116	0.142	2.016	0.201	1.969
K	1.852	1.819	1.928	1.816	1.827	1.810	1.871	1.825	1.854	1.756	1.756	
Fe												
Fe+Mg+Mn	0.243	0.239	0.267	0.309	0.275	0.267	0.285	0.282	0.278	0.349	0.349	

D.D.H. MM -19 at 1673 feet (cont'd.)

D.D.H. MM-19 at 2345 feet

Wt. %	3	4a	4b	4c	5	6	7	1	2	3a
SiO ₂	39.02	38.23	38.14	38.74	37.81	36.76	36.43	37.42	37.82	38.97
TiO ₂	2.89	3.62	3.63	3.72	4.34	4.17	4.40	4.06	3.19	2.99
Al ₂ O ₃	15.27	15.08	15.18	14.96	15.13	13.79	13.74	15.43	14.92	15.60
Cr ₂ O ₃	0.00	0.03	0.02	0.00	0.00	0.07	0.00	0.08	0.06	0.00
FeO	8.71	11.98	10.85	11.87	10.21	15.58	15.35	8.10	9.07	7.33
MnO	0.03	0.02	0.00	0.00	0.01	0.12	0.04	0.04	0.00	0.02
MgO	17.81	15.54	16.39	16.13	16.65	14.10	14.08	18.52	18.14	19.06
CaO	0.11	0.09	0.04	0.06	0.05	0.08	0.14	0.08	0.06	0.11
Na ₂ O	0.49	0.51	0.50	0.55	0.50	0.69	0.44	0.50	0.42	0.63
K ₂ O	9.97	9.76	9.63	9.64	9.65	9.28	9.11	9.84	9.68	9.85
Total	94.30	94.86	94.38	95.67	94.35	94.64	93.73	94.07	93.36	94.56

Numbers of ions on the basis of 22 oxygens

Si	5.715	8.000	8.000	8.000	8.000	8.000	8.000	8.000	8.000	8.000
Al	2.285	2.341	2.360	2.327	2.416	2.426	2.435	2.497	2.384	2.344
Al	0.352	0.290	0.286	0.255	0.218	0.039	0.039	0.178	0.227	0.324
Ti	0.318	0.403	0.404	0.410	0.482	0.476	0.505	0.449	0.356	0.326
Cr	-----	5.630	0.004	5.612	5.639	5.628	5.702	5.717	5.698	5.666
Fe ²⁺	1.067	1.483	1.342	1.454	1.261	1.976	1.961	0.996	1.126	0.890
Mn	0.004	0.003	-----	-----	0.001	0.015	0.005	0.005	-----	0.002
Mg	3.889	3.429	3.613	3.521	3.666	3.187	3.206	4.060	4.015	4.123
Ca	0.017	0.014	0.006	0.009	0.008	0.013	0.023	0.013	0.010	0.017
Na	0.139	2.020	0.146	2.004	1.966	0.143	2.011	0.143	2.002	0.177
K	1.863	1.843	1.817	1.801	1.818	1.795	1.775	1.846	1.834	1.824
Fe	-----	-----	-----	-----	-----	-----	-----	-----	-----	-----
Fe+Mg+Mn	0.215	0.302	0.271	0.292	0.256	0.382	0.379	0.197	0.219	0.177

D.D.H. MM-19 at 2345 feet (cont'd.)

D.D.H. MM-20 at 772 feet

Wt. %	3b	4	5	1a	1b	2	3	4	5	6a
SiO ₂	37.99	38.62	38.21	38.17	39.27	38.68	38.69	37.98	40.02	39.53
TiO ₂	3.17	2.93	3.16	3.92	3.44	3.24	3.34	4.27	2.03	1.84
Al ₂ O ₃	14.68	15.60	15.44	14.48	14.41	14.43	13.96	14.21	14.55	13.20
Cr ₂ O ₃	0.00	0.01	0.00	0.00	0.00	0.03	0.02	0.00	0.00	0.00
FeO	7.39	8.08	7.92	9.67	9.19	9.83	10.27	9.49	7.90	10.07
MnO	0.00	0.00	0.00	0.00	0.03	0.00	0.00	0.04	0.00	0.03
MgO	19.16	19.05	18.88	18.06	18.88	18.30	18.06	18.00	20.12	19.80
CaO	0.05	0.09	0.11	0.05	0.06	0.02	0.07	0.05	0.06	0.02
Na ₂ O	0.38	0.49	0.61	0.24	0.62	0.59	0.50	0.44	0.44	0.47
K ₂ O	9.90	9.73	9.63	9.55	9.82	9.69	9.73	9.60	9.72	9.53
Total	92.72	94.60	93.96	94.14	95.72	94.81	94.64	94.08	94.84	94.49

Numbers of ions on the basis of 22 oxygens

Si	5.640	8.000	8.000	5.627	8.000	5.671	8.000	5.611	8.000	5.810
Al	2.360	2.380	2.399	2.373	2.315	2.329	2.302	2.389	2.212	2.190
Al	0.209	0.296	0.268	0.144	0.143	0.165	0.121	0.086	0.269	0.097
Ti	0.354	0.321	0.348	0.435	0.375	0.357	0.370	0.474	0.221	0.203
Cr	-----	5.721	5.734	5.713	-----	5.708	0.002	5.723	-----	5.880
Fe ²⁺	0.918	0.983	0.971	1.192	1.113	1.205	1.265	1.173	0.956	1.238
Mn	-----	-----	-----	-----	0.004	-----	-----	0.005	-----	0.004
Mg	4.240	4.133	4.125	3.969	4.074	4.000	3.965	3.964	4.338	4.338
Ca	0.008	0.014	0.017	0.008	0.009	0.003	0.011	0.008	0.009	0.003
Na	0.109	0.138	0.173	0.069	0.174	0.168	0.143	0.126	1.926	0.134
K	1.875	1.807	1.801	1.796	1.814	1.812	1.828	1.809	1.794	1.787
Fe	-----	-----	-----	-----	-----	-----	-----	-----	-----	-----
Fe+Mg+Mn	0.178	0.192	0.190	0.231	0.214	0.232	0.242	0.228	0.180	0.222

D.D.H. MM-20 at 772 feet (cont'd.)

D.D.H. MM-21 at 471 feet

Wt. %	6b	7a	7b	1	2	3	4	5a	5b
SiO ₂	39.74	38.56	39.28	38.30	37.43	36.70	37.07	36.39	38.15
TiO ₂	1.95	3.49	2.68	4.02	4.09	4.72	4.51	4.60	3.94
Al ₂ O ₃	14.24	14.72	14.18	12.68	13.27	13.15	13.03	13.18	12.99
Cr ₂ O ₃	0.00	0.01	0.10	0.00	0.00	0.00	0.01	0.00	0.00
FeO	9.09	8.50	7.96	14.45	14.82	15.46	15.47	16.10	15.74
MnO	0.00	0.04	0.00	0.00	0.08	0.09	0.10	0.10	0.02
MgO	19.92	19.33	19.37	15.64	14.74	14.74	14.71	14.25	14.90
CaO	0.00	0.07	0.05	0.02	0.05	0.08	0.10	0.05	0.05
Na ₂ O	0.37	0.34	0.13	0.48	0.45	0.22	0.35	0.35	0.53
K ₂ O	9.82	9.56	9.67	9.79	9.58	9.26	9.31	9.28	9.49
Total	95.13	94.62	93.42	95.38	94.51	94.42	94.66	94.30	95.81

Numbers of ions on the basis of 22 oxygens											
Si	5.770	8.000	8.000	5.724	7.958	8.000	5.612	5.555	7.927	5.702	7.990
Al	2.230	2.377	2.226	2.234	2.341	2.353	2.325	2.372	2.288		
Al	0.208	0.153	0.231	0.000	0.024	0.000	0.000	0.000	0.000	0.000	0.000
Ti	0.213	0.383	0.296	0.452	0.465	0.539	0.514	0.528	0.443	0.443	0.443
Cr	-----	5.836	0.012	-----	-----	-----	0.001	-----	-----	-----	5.732
Fe ²⁺	1.104	1.037	0.979	1.806	1.874	1.963	1.959	2.056	1.967	1.967	
Mn	-----	0.005	-----	-----	0.010	0.012	0.013	0.013	0.003	0.003	
Mg	4.312	4.202	4.245	3.485	3.322	3.335	3.320	3.243	3.319	3.319	
Ca	-----	0.011	0.008	0.003	0.008	0.013	0.016	0.008	0.008	0.008	
Na	0.104	1.923	0.037	0.139	2.009	0.132	0.103	0.104	1.919	0.154	1.971
K	1.819	1.779	1.814	1.867	1.848	1.793	1.798	1.807	1.807	1.807	
Fe											
Fe+Mg+Mn	0.204	0.198	0.187	0.341	0.360	0.370	0.370	0.387	0.372	0.372	

D.D.H. MM-24 at 817 feet

Wt. %	1	2	3	4a	4b	5a	5b	6a	6b
SiO ₂	39.28	37.88	37.44	38.94	37.58	36.93	36.65	36.87	38.01
TiO ₂	3.12	3.96	4.12	3.31	3.67	0.62	0.62	1.53	3.20
Al ₂ O ₃	13.59	14.56	14.56	13.87	14.04	18.38	18.86	17.91	16.03
Cr ₂ O ₃	0.04	0.00	0.00	0.02	0.00	0.00	0.02	0.00	0.04
FeO	7.88	10.17	10.22	9.65	10.05	9.49	9.72	9.23	8.20
MnO	0.03	0.05	0.00	0.01	0.01	0.05	0.04	0.01	0.08
MgO	20.39	17.65	17.86	19.26	18.44	17.30	17.19	18.16	19.18
CaO	0.10	0.02	0.10	0.04	0.07	0.02	0.10	0.09	0.15
Na ₂ O	0.56	0.40	0.59	0.61	0.61	0.67	0.52	0.44	0.67
K ₂ O	9.91	9.76	9.51	9.88	9.79	10.10	10.21	10.23	9.67
Total	94.90	94.45	94.40	95.59	94.26	93.56	93.93	94.47	95.23

Numbers of ions on the basis of 22 oxygens

Si	5.711	8.000	5.538	8.000	5.668	8.000	5.483	8.000	5.424	8.000	5.512	8.000
Al	2.289	2.405	2.462	2.332	2.426	2.517	2.571	2.576	2.576	2.576	2.488	2.488
Al	0.040	0.130	0.076	0.048	0.029	0.700	0.722	0.529	0.251	0.529	0.251	0.251
Ti	0.341	0.440	0.458	0.362	0.409	0.069	0.069	0.169	0.349	0.169	0.349	0.349
Cr	0.005	5.767	5.718	0.002	5.768	5.764	5.783	5.799	5.817	5.817	5.817	5.755
Fe ²⁺	0.958	1.256	1.264	1.175	1.247	1.178	1.204	1.136	0.994	1.136	0.994	0.994
Mn	0.004	0.006	0.000	0.001	0.001	0.006	0.005	0.001	0.010	0.001	0.010	0.010
Mg	4.419	3.886	3.938	4.179	4.077	3.829	3.796	3.982	4.146	3.982	4.146	4.146
Ca	0.016	0.003	0.016	0.006	0.011	0.003	0.016	0.014	0.023	0.014	0.023	0.023
Na	0.158	2.012	0.169	1.980	0.175	2.039	0.149	2.095	2.060	0.126	2.060	2.001
K	1.838	1.839	1.795	1.835	1.853	1.913	1.930	1.920	1.789	1.920	1.789	1.789
Fe												
Fe+Mg+Mn	0.178	0.244	0.243	0.219	0.234	0.235	0.241	0.222	0.193	0.222	0.193	0.193

Wt. %	D.D.H. MM-28 at 548 feet			D.D.H. MM-28 at 895 feet			D.D.H. MM-28 at 1219 feet			
	1	2	3a	3b	4	1	2	1	2	3a
SiO ₂	37.39	36.55	38.28	38.22	38.06	38.18	36.61	37.50	37.37	38.41
TiO ₂	2.63	2.80	3.00	2.70	2.89	2.78	2.85	2.71	3.89	2.76
Al ₂ O ₃	15.84	15.21	14.77	14.81	14.82	16.44	15.43	14.30	14.95	14.23
Cr ₂ O ₃	0.03	0.01	0.03	0.04	0.04	0.23	0.30	0.06	0.00	0.00
FeO	6.64	6.52	6.92	6.93	7.52	9.50	9.39	6.22	8.45	7.03
MnO	0.03	0.01	0.06	0.11	0.00	0.00	0.04	0.00	0.02	0.04
MgO	19.77	18.97	19.75	20.20	19.05	18.12	16.90	19.39	18.38	19.67
CaO	0.16	0.07	0.05	0.10	0.07	0.09	0.04	0.05	0.00	0.00
Na ₂ O	0.50	0.34	0.44	0.46	0.63	0.46	0.68	0.24	0.27	0.40
K ₂ O	10.21	10.00	9.85	9.86	9.85	10.18	9.85	9.74	9.79	9.76
Total	93.20	90.48	93.15	93.43	92.93	95.98	92.09	90.21	93.12	92.30
Numbers of ions on the basis of 22 oxygens										
Si	5.521	8.000	5.642	5.621	8.000	5.643	8.000	5.688	8.000	5.710
Al	2.479	2.444	2.358	2.379	2.357	2.469	2.453	2.312	2.445	2.290
Al	0.278	0.281	0.208	0.189	0.233	0.338	0.302	0.245	0.174	0.204
Ti	0.292	0.320	0.333	0.299	0.322	0.303	0.325	0.309	0.435	0.309
Cr	0.004	5.748	0.003	0.005	5.787	0.026	0.036	0.007	5.735	5.751
Fe ²⁺	0.820	0.829	0.853	0.852	0.933	1.151	1.190	0.789	1.050	0.874
Mn	0.004	0.001	0.007	0.014	-----	-----	0.005	-----	0.003	0.005
Mg	4.352	4.298	4.339	4.429	4.211	3.913	3.817	4.384	4.072	4.359
Ca	0.025	0.011	0.008	0.016	0.011	0.014	0.006	0.008	-----	-----
Na	0.143	2.092	0.126	0.131	1.997	0.129	2.025	0.071	1.964	1.934
K	1.923	1.939	1.852	1.850	1.863	1.881	1.904	1.885	1.856	1.851
Fe										
Fe+Mg+Mn	0.158	0.162	0.164	0.161	0.181	0.227	0.237	0.152	0.205	0.167

D.D.H. MM-28 at
at 1219 feet

D.D.H. MM-28 at 1844 feet

Wt. %	3b	1	2
SiO ₂	39.54	37.47	37.92
TiO ₂	2.53	3.86	3.87
Al ₂ O ₃	16.10	15.39	15.60
Cr ₂ O ₃	0.01	0.00	0.03
FeO	6.53	8.39	7.79
MnO	0.04	0.00	0.04
MgO	16.81	17.97	18.60
CaO	0.00	0.07	0.10
Na ₂ O	0.33	0.52	0.74
K ₂ O	9.94	9.62	9.69
Total	91.83	93.29	94.38

Numbers of ions on the basis of 22 oxygens

Si	5.855	8.000	5.552	8.000	5.541	8.000
Al	2.145		2.448		2.459	
Al	0.665		0.240		0.228	
Ti	0.282		0.430		0.425	
Cr	0.001	5.472	-----	5.679	0.003	5.665
Fe ²⁺	0.809		1.040		0.952	
Mn	0.005		-----		0.005	
Mg	3.710		3.969		4.052	
Ca	-----		0.011		0.016	
Na	0.095	1.972	0.149	1.979	0.210	2.032
K	1.878		1.819		1.806	
Fe						
Fe+Mg+Mn	0.179		0.208		0.190	